Conjugated Poly-ynes and Poly(Metalla-ynes) Incorporating Thiophene-based Spacers for Solar Cell (SC) Applications[#]

Muhammad S. Khan[1]*, Mohammed K. Al-Suti[1], Jayapal Maharaja[1], Ashanul Haque[1], Rayya Al-Balushi[1] and Paul R. Raithby[2]*

[1]*Department of Chemistry, Sultan Qaboos University, P.O. Box 36, Al Khod 123, Sultanate of Oman. *E-mail:msk@squ.edu.om*

[2]*Department of Chemistry, University of Bath, Claverton Down, Bath BA2 7AY, UK. *E-mail:p.r.raithby@bath.ac.uk*

Abstract

Solar cells (SCs) are of considerable current research interest because of their potential as a clean alternative to fossil fuels. Researchers across the globe are developing novel polymeric materials with enhanced power conversion efficiency (PCE). Conjugated poly-ynes and poly(metalla-ynes) incorporating late transition metals and thiophene-based spacers have played a very important role in this strategic area of materials research. The performance of the SCs can be optimized by varying the conjugated spacers and/or the metal ions along the polymer backbone. Therefore, an analysis of structure-photovoltaic property relationships in poly-ynes and poly(metalla-ynes) is desirable as a guide for the development of new functional materials for use in SCs. Keeping the importance of this strategic topic in mind, herein we present a brief review on conjugated poly-ynes and poly(metalla-ynes) incorporating thiophene-based spacers that have potential SC applications. Attempts have been made to correlate the photovoltaic performance of the SCs to the chemical structure of thiophene-incorporated poly-ynes and poly(metalla-ynes). The performance of SCs is also strongly influenced by other factors such as morphology and device structure.

Keywords: Metalla-yne, Thiophene, Thienyl, Band gap, Power conversion efficiency.

Highlights

- Thiophene-based conjugated poly-ynes and poly(metalla-ynes) have been reviewed.
- The materials possess low band gap with broad absorption range.
- Poly(platina-ynes) have lower PCE values compared to their organic counterparts.
- The performance depends on chemical structure, morphology and device architecture.

[#]*Dedicated to the memory of late Professor the Lord Lewis of Newnham for his pioneering contribution in the field of transition metal clusters, coordination chemistry and organometallic polymer chemistry.*

1. Introduction

Rising global demand for clean and sustainable energy sources has put considerable pressure on the scientific community for the development of efficient and low-cost renewable energy sources [1]. Solar energy has emerged as a potential non-contaminating alternative energy source to meet the increasing demand [2]. In fact, the planet Earth receives more energy from the sun each second than is required to meet the needs of mankind for one year [3]. However, the conversion of solar energy into electrical energy is a daunting task in the context of industrial and practical applications. The conversion is achieved by using specially designed devices embedded within cells called solar cells (SCs). SC devices are comprised of different components which govern the overall performance of the cells. These include electrodes, interfacial layers, and active materials composed of donor (D) and acceptor (A) components [4]. All of these components contribute to the overall efficiency of a SC. However, most of the research has been dedicated to the development of novel donor materials. In the past two or three decades there has been a large volume of research relating to the development of donor materials [5], particularly conjugated poly-ynes and poly(metalla-ynes) incorporating a variety of spacer groups because of their good absorption profile, energy conversion ability, processability and low-cost [4b, 4c, 6]. Poly-ynes incorporating several carbocyclic and heterocylic spacers [7], for example, benzene [8], anthracene [9], 2,1,3-benzothiadiazole (BTD) [10], cyclopentathiophene [11], thienopyrazine [12], dithienothiophene [13], bithiazole [14] and dithienopyrrole [15], etc. have been synthesized and assessed for SC applications. Heterocyclic spacers are considered more efficient compared to their purely carbocyclic counterparts in producing efficient SCs. Among the heterocyclic spacers, thiophene-based materials have been extensively studied and used for making low band-gap (E_g) conjugated polymers [16], which is one of the prime requirements for efficient SCs. Thiophene-based spacers are also known to lower the polarity and enhance the solubility of the polymer materials [17]. It is a well-established fact now that the incorporation of heavy transitional metals along polymer backbone induces large spin-orbit coupling and imparts novel opto-electronic (OE) properties to the materials [7c, 18]. Researchers have exploited the novel photo-physical properties and discovered the photovoltaic (PV) effect of organometallic poly-ynes and successfully demonstrated the utility of heavy metal incorporation into the poly-yne framework. Historically, the work on metal-based SC started around two decades ago when Köhler et al. [8a] reported a Pt(II)

poly-yne-based SC with a PCE of ~ 0.6%. The efficiency was too low for commercial application, but this finding added a new dimension to the research and the development of conjugated poly(metalla-ynes) for SC applications. Many organic and organometallic (metal-based) donor materials have been reported as active layers for SC applications [7d, 14, 16b, 19], a few with remarkably high efficiencies. For example, Zhan et al. [20] achieved 3.8 % PCE for the organic oligo-yne incorporating cyclopentadithiophene (CDT) as a central spacer unit. Likewise, Kumar et al. [16b] reported A-π-D-π-A based oligo-yne, with extended absorption in the NIR region giving PCE of 3.65 % and 5.24 %, depending on solvents THF and pyridine-THF respectively. Baek et al. [4b] reported a poly(platina-yne) incorporating thienothiophene, having enhanced interaction between D and A units in the polymer backbone and obtained a PCE of 4.13 % with [6,6]-phenyl-C_{71}-butyric acid methyl ester ($PC_{71}BM$). Wong et al. [17f] reported poly(platina-yne) incorporating a thiadiazole spacer with oligothiophene units at the two ends. A PCE of 2.50 % was achieved for a material with three thiophene rings at each end. For further details of other recently reported SCs, the interested readers are referred to refs [7d, 14, 16b, 19], [17e, 17f, 21]. The device performance of polymer SCs is greatly affected by various parameters including the chemical structures [22], the optical band gap (E_g) [23], the charge mobilities [22a], the absorption co-efficients [10], the accessibility of triplet excitons (a bound electron-hole pair) [24], the molecular weights [25], the blend film morphologies [4b, 26] and the connectivity order of the ligands in co-polymers. Hence, the PV performance of the SCs can be modified by changing all these parameters, which are associated with the materials. Many poly-ynes with narrow E_g (< 1.9–2.0 eV), absorptions in the longer wavelength region (extended IR region) and good to moderate PCEs have been reported [17e, 17f, 21]. In most of the cases, researchers focused on developing novel donor materials and optimizing their properties by incorporating late transition metals in a way that resulted in efficient SCs. Considering these facts, herein we present a brief review on thiophene-based poly-yne and poly(metalla-yne) materials for SC application. Attempts have been made to forge a link between the PV performance and the structure of poly-ynes and poly(metalla-ynes) incorporating thiophene spacers. This will give a broad overview to researchers for the design and development of novel donor materials for applications in SCs.

2. Basics of SCs

2.1 Structure of SCs

Several leading articles and monographs are available describing the structure of SCs and the mechanism by which they work [27]. However, for the sake of general readers and new researchers in this area, we present a brief view of the basic structure of SCs, their performance parameters and working mechanism. Fig. 1a depicts a basic SC architecture consisting of a transparent anode made of indium tin oxide (ITO) or fluorine-doped tin oxide (FTO), followed by an interfacial layer [28]. The interfacial layer plays a very important role in the device performance and is known to enhance V_{oc} and FF by optimizing solar absorption and supressing charge carrier recombination [29]. Poly(3,4-ethylenedioxy thiophene) poly(styrenesulfonate) (PEDOT:PSS) is the most widely used interfacial layer. It acts as an efficient hole transport layer (HTL)/electron-blocking layer [30], due to its good conductivity, easy processability, transparency (> 80 %), insolubility in common organic solvents and matching work function (~ -5.1 eV) with the fermi level of a wide E_g polymer in making good Ohmic contact at the anode/BHJ interface [31]. Then comes a more vital active layer, which absorbs light and supplies excitons. This is the layer where most of the modifications have been made so far. Generally, the active layer includes a p-type (D) and an n-type (A) material, which functions as a hole transporting material and an electron accepting material, respectively. It should be noted that the surface morphology of the active layer of SC can be modified by using different solvents, additives and by the application of thermal annealing. Hence, the parameters like the open-circuit potential (V_{oc}) and short-circuit current density (J_{sc}) (*discussed in next section*), which determine the PV efficiency, can be modified. Similarly, the concentration of acceptor material in the active layer also plays a crucial role [16b]. Finally, there is a cathode made up of a metal such as aluminium and is separated by a second interfacial layer (electron transport layer, ETL). Numerous n-type materials like LiF, cesium carbonate (Cs_2CO_3) [32], TiO_x [33], doped TiO_2 [34], ZnO [35], ZnO as a self-assembled monolayer [36], graphene [37] and CrO_x [38] have been employed as ETL in SC. Combination of LiF with C_{60} [39] and other metal oxides e.g. CuO_x [40] have also been used as ETLs in SC. These wide E_g ETL materials provide a barrier for excitons [41].

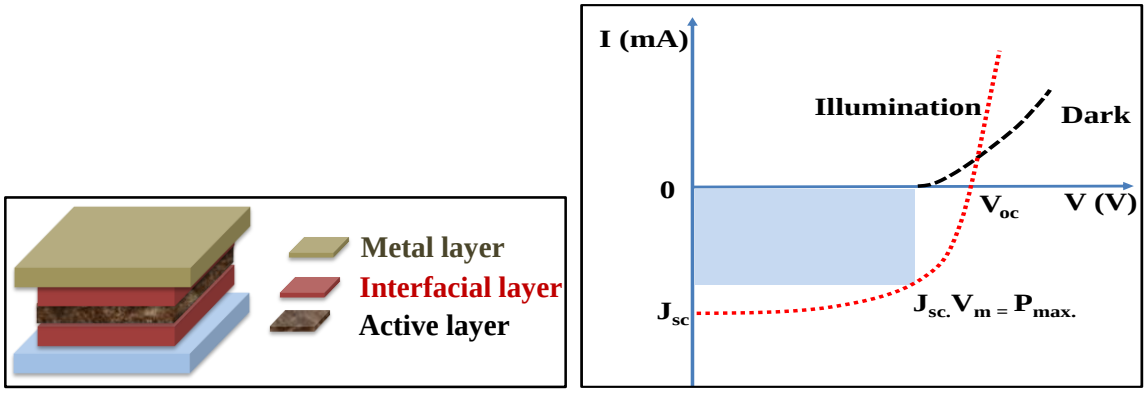

Fig. 1. (a) Schematic diagram of SC architecture and (b) A typical J-V characteristics curve (Reproduced with permission from Ref. [42]).

2.2 Performance parameters

Fig. 1b illustrates the current (I)–voltage (V) characteristics of the SC in the dark and under illumination [42]. The J_{sc} is given by the maximum generated photo-current. The electron and hole transport efficiency of the active layer affects the J_{sc} value in the organic polymer based Blend/Bulk-Heterojunction (BHJ). Generally, the unbalanced charge transport is caused by the high electron mobility rather than the hole mobility [16b]. V_{oc} is contributed to the open circuit of the SC (voltage at zero current). The energy difference between the highest occupied molecular orbital (HOMO) of p-type donor and the lowest unoccupied molecular orbital (LUMO) of n-type acceptor limits the V_{oc} [17e, 43]. The V_{oc} is also influenced by the parallel resistance (shunts) [44]. The fill factor (FF) (Eq.1) is the ratio of actual maximum power output of the SC to its theoretical power output [45]. Theoretically, the maximum value of FF is 1.0. However, it is difficult to achieve a FF above 0.83 in practice.

$$FF = \frac{J_m \times V_m}{J_{sc} \times V_{oc}} \quad (Eq.1)$$

The PCE (η) (Eq. 2) is defined as the ratio of the electrical power density to the incident solar power density (P). P is the value of spectral intensity matching the sun's intensity on the earth's surface at an angle of 48.2° (equivalent to AM 1.5 spectrum) [42, 46].

$$\eta = \frac{J_m \times V_m}{P} \quad (Eq.2)$$

$$\eta = \frac{J_m \times Voc \times FF}{P} \quad (Eq.3)$$

The PCE can also be measured as the incident photon to conversion efficiency (IPCE) (Eq. 4). It is the charge carriers collected at the electrodes divided by the number of incident photons falling on the device, which is also known as external quantum efficiency (EQE).

$$\text{IPCE } \% = \left(\frac{1240 \times \text{J}_{\text{sc}}}{\lambda \times I_{inc}}\right) \times 100 \ (Eq.\ 4)$$

where, J_{sc} = short-circuit current density, λ = wavelength, I_{inc} = the incident light power density. The short circuit photocurrents (J_{sc}) observed at different excitation wavelengths can be used to determine IPCE at different wavelengths.

2.3 The working mechanism of SCs

The conversion of solar energy into electrical energy by the SC involves four sequential steps [47], depicted in Fig. 2. The first step involves the formation of exciton by the absorption of photons followed by their diffusion into the D-A interfaces (step 2, Fig. 2). The excitons dissociate into charge carriers. Subsequently, the charges are collected by the anode and cathode (step 3 and 4, Fig. 2). Generally, excitation of an electron from the HOMO to the LUMO level occurs when the incident light energy is greater than the E_g of the semi-conducting material. This transition leaves behind the unoccupied valence state called a 'hole' [48]. The photon energy now exists in the exciton as the potential energy difference of excited electron-hole pair [49]. Other characteristics such as the absorption coefficient, absorption spectrum, absorbing layer thickness and internal multiple reflections also determine the fraction of absorbed photons. The internal electric field and concentration gradient are the main forces which contribute to the charge carriers transport. Field induced drift is dominant in most of the thin film (< 100 nm) devices whereas the concentration gradient is dominant in most of the thick devies. However, the excited electron also undergoes thermal relaxation to the LUMO level with release of heat as there is continuum of states above the LUMO level. In order to generate electricity, the exciton must be separated and collected by the respective electrode, which can be accomplished by introducting an electron-acceptor such as ([6,6]-phenyl-C_{61}-butyric acid methyl ester (PCBM) or $PC_{71}BM$ in the active layer. The electron-acceptor should have the low lying LUMO level so that the electron transfer from D → A becomes feasible. The electron and hole transport will be highly favourable when the energy difference between HOMO and LUMO of D and A, respectively, is greater than or equal to the exciton energy. The electron can also recombine easily with the hole owing to a very short life-time of the exciton. Therfore, the electron has

to be trapped as soon as the exciton is formed. To achieve this the distance between an exciton generation site and D/A interface should be 5-10 nm [31]. In addition, the D and A should be interconnected in 3D nanoscale phase separation for efficient dissociation and transportation of the charge carrier to the respective electrode to result in high PCE. In addition to the nanoscale surface morphology of blend film, both the light-harvesting and charge-transporting properties are affected by orientation of the backbone of the polymer donor with respect to the substrate [31, 50]. Generally, the active layer is prepared by a casting (printing or coating method) technique from the solvent (for e.g. dicholorobenzene, toluene, chloroform etc.) having dissolved D and A in an appropriate ratio.

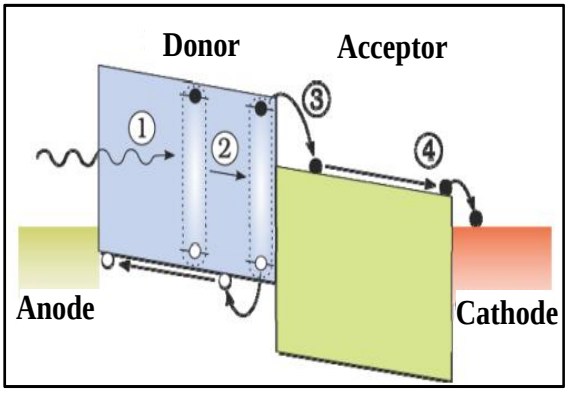

Fig. 2. A schematic diagram of working mechanism of SCs. (Reproduced with permision from Ref. [51]).

3. Thiophene and its derivatives

Thiophene and its derivatives are widely used building blocks for conjugated poly-ynes and poly(metalla-ynes) due to their excellent OE properties and good thermal stability. Better PCE can be achieved using alternating D-A conjugated polymers having low-E_g and high crystallinity in thin films [4c, 21b]. Since thiophene derivatives are capable of lowering E_g by extending π-electron delocalized systems in the chain, they can be used as electron donor and hole transporting materials [52]. Thiophene derivatives such as 3,4-ethylenedioxythiophene (EDOT), poly(3-hexylthiophene) (P3HT), thienopyrazine, dithienopyrrole, thieno[3,4–*b*] thiophene and benzothiophene are some of the commonly employed spacer groups used for this purpose [53]. **Chart 1** depicts some of the important thiophene-based spacers assessed for the development of SCs. In addition, the properties of thiophenes can be easily tuned by modifying their structure. For example, the solubility of thiophene can be increased by anchoring solubilizing moieties on the ring [7b, 11a]. Not surprisingly, when thiophene was incorporated as a spacer into the poly(metalla-yne) polymer, it gave a relatively high PCE

(4.93%) [10]. Furthermore, the combination of an electron-donating thiophene and an electron-accepting BTD is also a good strategy to lower the E_g of the polymers (< 2.0 eV) for enhancing the PCE [10]. Similarly, fused oligothiophenes such as thienothiophene and dithienophene are planar and the resultant high π-conjugation coupled with high thermal stability, a good absorption profile, interchain π-stacking and enhanced charge carrier mobility makes them promising polymer materials for SC application [54].

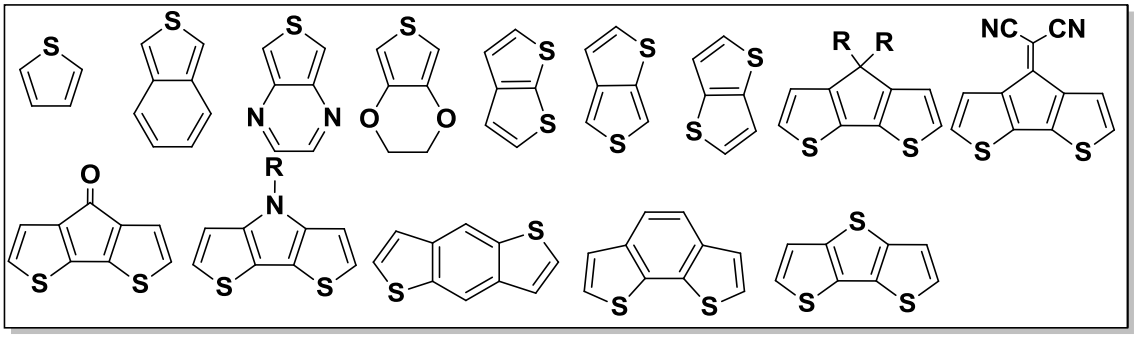

Chart 1: Some thiophene-based spacers used for SCs.

4. Poly-ynes incorporating thiophene-based spacers as active layers for SCs

4.1 Conjugated oligo-ynes and poly-ynes

Several organic poly-ynes with low-E_g have been reported as donor materials for SC applications [12c, 55]. However, the PCE of all low-E_g poly-yne materials are lower than P3HT (**OP1**) [12b, 56]. In order to overcome this limitation, it is necessary to keep V_{oc} as high as possible, which is considered as a great challenge [55a]. Generally, the energy difference between the p-type donor and n-type acceptor creates V_{oc}. Therefore, the V_{oc} and hence PCE can be increased by lowering the HOMO energy level of the p-type polymer.

Polyalkyl thiophenes (PATs) are known to possess intriguing OE properties. These polymers were developed to improve the solubility of parent thiophene-based polymers [57]. For detailed synthetic protocol and physico-chemical properties of PATs, readers are encouraged to read comprehensive reviews by McCullough and others [58]. Among the PATs, P3HT (**OP1)** is a classical polymer used in SCs. It exhibits a good absorption profile in thin film state (450 nm-600 nm), high electrical conductivity, and high field-effect mobility [59]. In addition to these novel materials properties, the self-organization capacity, high hole mobility and low-E_g of **OP1** make it a remarkable material for SC applications [24, 60]. The intensity of absorption in thin film of **OP1** decreased as PCBM concentration increased, which reveals the necessity of having a thick active layer of **OP1** in SC in order to

have equivalent absorption [58d, 61]. The crystallinity of **OP1** is strongly affected by an increase in the PCBM concentration in the thin film [62]. In addition increase in concentration of PCBM in the thin film of blend of **OP1** and PCBM causes decrease in hole mobility and increase in electron mobility [63]. Therefore, it is necessary to optimize the blend ratio of polymer and PCBM in order to make a potentially active layer for achieving high PCE in SC. The amount of fullerene required for making blend films is less for **OP1** and PCBM blend compared to other polymer blends such as poly(phenylenevinylene) (PPV) and poly[*N*-11′′-henicosanyl-2,7-carbazole-alt-5,5-(4′,7′-di-2-thienyl-2′,1′,3′-benzothiadiazole)] (PCDTBT). Thermal annealing of the blended thin film of **OP1** and PCBM also enhances the solar cell performance, which is attributed to increase in charge transport due to increased crystallinity and formation of interconnected fibrils of **OP1** by thermal annealing [64].

OP1 and some related conjugated oligo-ynes and poly-ynes incorporating thiophene and its derivatives are given in **Chart 2**. When a device based on **OP1** was illuminated with light, a high J_{sc} of up to 10 mA/cm^2 and high PCE was achieved [28a, 65]. The effective SC performance of **OP1** is mainly caused by its tendency to self-organize in a lamellar microstructure [66], which leads to red shift of the absorption spectrum and charge carrier mobility. Woo et al. [66] reported an extensive study of the regio-regularity of the polymer on device performance. They reported that efficient SC can be achieved with 86% regio-regular **OP1**. This type of **OP1** also favors thermally stable devices, which can be ascribed to phase segregation of PCBM and gave a PCE of 3.9%. In addition, structural properties of **OP1** also have a remarkable effect on SC performance. When **OP1** nanofibrils were added to the **OP1**:PCBM composite film, enhanced optical absorption and hole transport properties were observed, because of the reinforced **OP1** networks and increased crystallinity [67]. The introduction of an ethynylene unit increases the V_{oc} of SC by raising the oxidation potential of the polymer [55b, 68]. A reduction in the HOMO energy level by 0.3 eV was also observed in a poly-yne consisting of alternating ethynylene and 4,3'-dihexyl-2,2'-bithien-5,5'-diyl units **OP2** compared to **OP1** [68]. It was reported that the electron-withdrawing ethynylene unit was responsible for lowering the HOMO level. BHJ SCs based on such polymeric material gave a PCE of 1.13%. The PCE of the device was found to vary with changes in parameters including the ratio of D and A, acceptor concentration and aggregation state of the polymers. For instance, a 1:1 combination of blend film with PCBM showed a J_{sc} of 1.84 mA/cm^2 while with ratios of 1:2 an 1:4, values of 2.6 and 3.1 mA/cm^2, respectively,

were obtained. The **OP2**:PCBM (1:4) blend film displayed an EQE of 42% at 450 nm, while it was 24% at 470 nm and 37% at 450 nm for the blend film of 1:1 and 1:2 ratio, respectively. However, very low FF (0.28-0.36) was shown by all combinations, which limited the overall performance, probably due to hindrance of hole mobility by the absence of aggregates. Although the introduction of an ethynyl unit in the polymer backbone lowers the HOMO energy level, its position also plays a vital role in achieving a low HOMO energy level as reported by Du et al. [69] Changing the position of ethynyl unit may possibly alter the HOMO and LUMO energy levels. However, it is challenging to predict the position which can offer lowest HOMO energy level. The poly-yne **OP3-OP6** (E_g = 1.76-1.97 eV) showed high V_{oc} in the range of 0.84-0.94 V. The best PCE of 1.6 % (V_{oc} = 0.94, J_{sc} = 4.2 mA/cm^2 and FF = 0.40) was achieved with the poly-yne containing an ethynylene unit between the BTD and the thiophene **OP6** compared with other poly-ynes **OP3-OP5**. The high V_{oc} compared to other poly-ynes was due to its lowest-lying HOMO energy levels. The EQE covering broad range from 300 to 750 nm was shown by the poly-yne **OP3-OP6** in the range of 18 %-45 %.

A thiophene moiety flanked by BTD units or vice-versa (**OP7** and **OP8)** resulted in thermally stable oligo-ynes [55b]. This type of oligo-yne is known to create a D-A-D-like system, which has the ability to lower E_g and enhance the co-planarity along the molecule [70]. Furthermore, the presence of a BTD unit was found to offer well-organized crystal structures [71] as well as providing a site for ring modification [72]. **OP7** having two thiophene units was found to show a better absorption profile than **OP8**. BHJ SCs with a 1:1 blend ratio, showed a V_{oc} of 0.89 V for **OP7** compared to 0.67 V for **OP8**. Oligo-yne **OP7** showed better performance (PCE of 0.56% at 1:1 ratio) compared to **OP8** (PCE = 0.13% at 1:1 ratio). A very similar PCE (0.66%) for the polymer based on **OP7** was reported by Ouyang and co-workers [19b]. However, another dithienyl- BTD containing poly-yne **OP9** showed a somewhat lower PCE (0.14%). They found that, upon annealing, the PCE of the materials decreased (zero at 110 °C). Furthermore, the active layer fabricated using chloroform was found to possess better PCE than the chlorobenzene counterpart. These two polymers are soluble, have low-E_g values (1.9 eV) compared to **OP8 (**Fig. 3**)** and other copolymer containing fluorene or carbazole with TBT and serve as efficient donor materials. Both thin film and polymeric solutions exhibited absorptions in visible region, which is an extra advantage of this material.

Zhan et al. [20] reported oligo-yne with different electron-rich aromatic bridges, such as C_6H_4, CDT and diphenyl(p-tolyl)amine **OP10-OP13** with PCE in the range of 2.36-3.28 %. Among them, CDT-bridged oligo-yne showed high PCE of 3.28 % attributed to its higher hole mobility, better absorption property and planar geometry which facilitates stronger intermolecular interaction and packing. The oligo-ynes **OP10-OP13** showed better performance compared to their corresponding Pt(II) counter parts. The presence of a central aryl bridge in place of the $Pt(PBu_3)_2$ unit caused a reduction in HOMO energy level and resulted in a high V_{oc}. A higher HOMO energy level resulting from the introduction of additional thiophene rings in oligo-yne **OP13** caused a reduction in V_{oc}. Oligo-yne **OP10-OP13** showed EQE in the range of 45-53 %, which indicates efficient power conversion.

In an attempt to increase the V_{oc} by raising the oxidation potential, some poly-ynes incorporating electron-rich thiophenes and electron-deficient aromatic units (**OP14-OP16, Chart 3**) were reported by Ashraf et al. [55a] These soluble π-conjugated organic polymers showed higher oxidation potentials and V_{oc} (0.72-0.82 V) values than the comparable derivatives without triple bonds (V_{oc} = 0.38-0.55 V) [11b, 73]. A similar trend was found for the E_g in which the polymer without C≡C bonds possessed a lower E_g compared to **OP14-OP16**. The blend ratio of 1:3 of **OP14-OP16** with PCBM gave J_{sc} in the range of 4.11-5.87 mA/cm^2, and FF in the range of 0.39-0.40. This led to an overall PCE of between 1.34-1.74%. A similar type of poly-yne containing alternating thienopyrazine and thiophene/alkylated benzene (**OP17-OP19**) was reported by the same group [12c]. Like the previous examples, these poly-ynes also showed low- E_g (1.57- 1.60 eV) and PCE in the range of 1.36-2.37%.

In contrast, **OP20-OP22 (Chart 3)** containing thiophene, bithiophene and EDOT spacers flanked by different alkylated aromatic rings showed PCE in the range of 0.43-0.92% at a blend ratio of 1:3 [26]. The high J_{sc} and low PCE were shown by the polymers **OP21** and **OP22**, respectively. The J_{sc} of the polymers were found to be limited by poor fluorescence quantum yields. Among all the reported polymers, **OP21** showed the best EQE (18%) with the highest J_{sc} (2.75 mA/cm^2). With an increasing amount of PCBM, better photo-induced electron transfer (PET) from the polymer to PCBM was also observed. **OP22** showed the lowest PCE (0.43%), which was ascribed to poor miscibility of the polymer.

An alternate combination of fused and non-fused spacer groups containing poly-yne **OP23** and **OP24** (**Chart 3**) gave PCEs of 0.85 and 2.40%, respectively, with a 1:1 blend ratio [74]. In addition to this, low HOMO levels (≤ -5.50 eV) of the polymers resulted in high V_{oc}

(0.90-0.92 V). Interestingly, upon annealing, an enhancement in PCE was observed for **OP24** while it decreased in **OP23**. The low J_{sc} and FF were attributed to the coarsening of the morphology, leading to reduction in diffusion and charge transport.

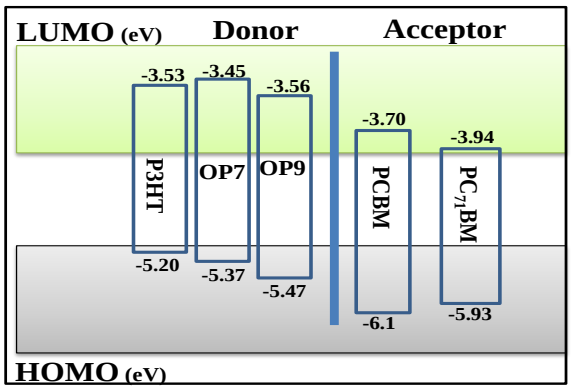

Fig. 3. Energy level diagram of **P3HT**, **OP7**, **OP9**, **PCBM** and **$PC_{71}BM$**.[19b]

A similar type of poly-yne (**OP25-OP28, Chart 4**) was reported by Daniel and co-workers [25, 75]. In these systems, the V_{oc} was found to be mainly influenced by the length of the chain and morphology. Furthermore, reduction in mobility of photo-generated charges were observed as the number of C≡C units was increased [65b]. PCE was maximised (1.21 %) for **OP25**, while it was 0.27% (minimum) for **OP27**. Poor SC performance of **OP27** compared to **OP17** was attributed to the lower molecular weight and higher number of C≡C units in backbone with longer dodecyl and octadecyl side chains.

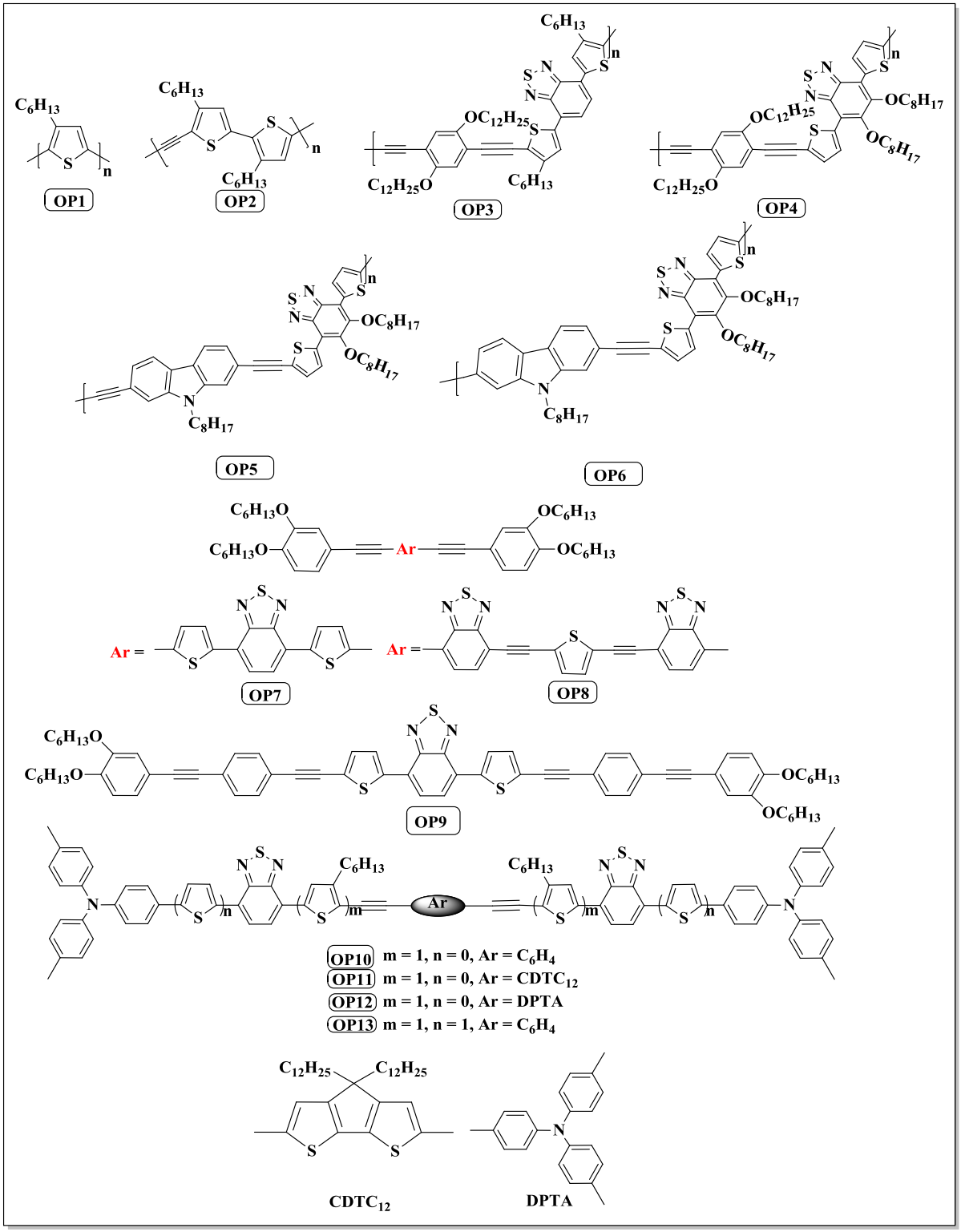

Chart 2: P3HT and some conjugated oligo-ynes and poly-ynes incorporating thiophene and its derivatives as active layers for SCs.

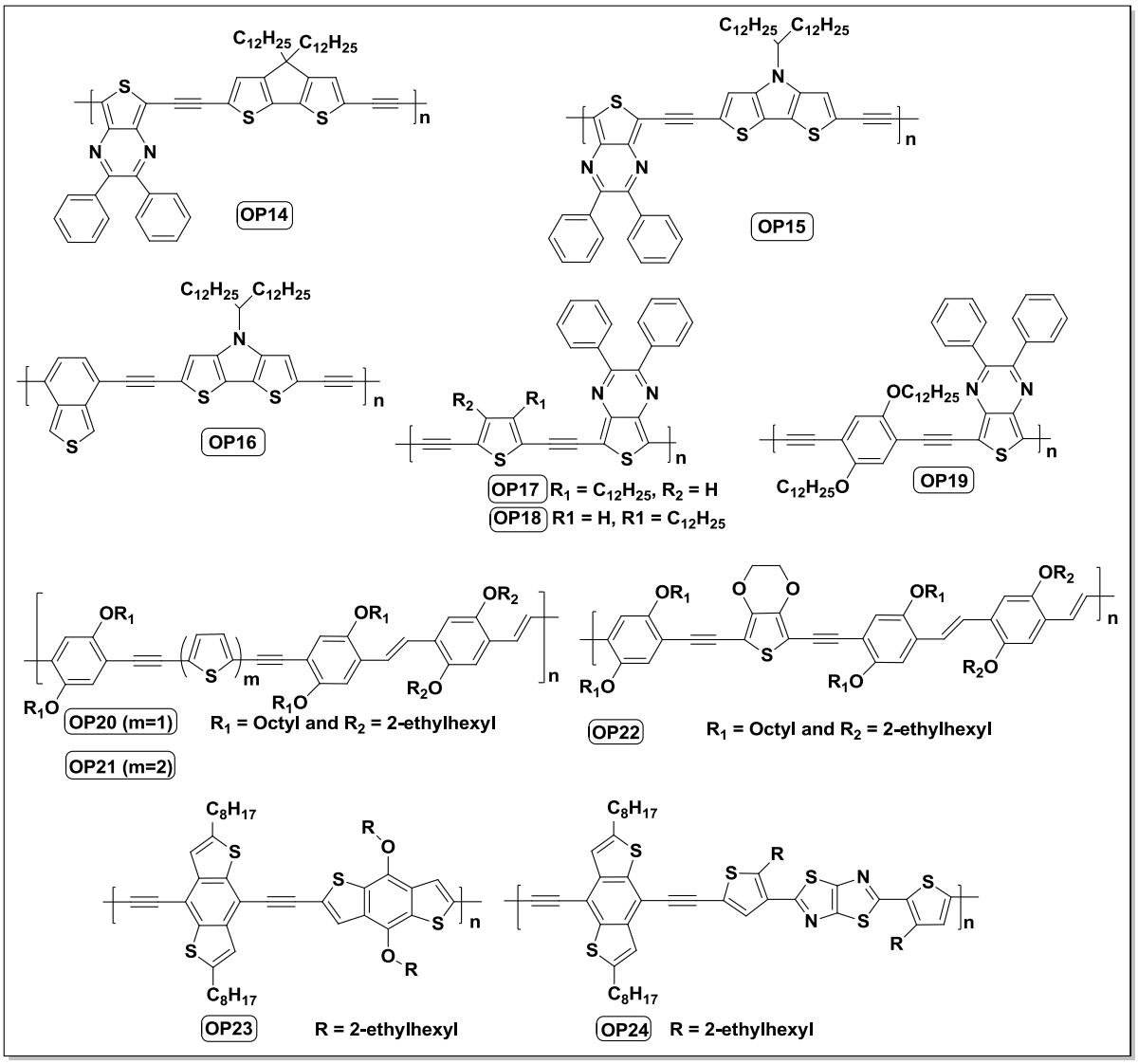

Chart 3: Organic poly-yne incorporating hybrid spacer containing thiophene**.**

Schanze et al. [7b] reported the SC active material **OP29** in which poly-(phenyleneethynylene)-based anionic conjugated polyelectrolytes act as electron donors and water-soluble cationic fullerene C_{60} derivatives as acceptors, respectively. They fabricated a layer-by-layer (LBL) film of the D-A system for photocells (PCs), which ultimately gives a control at molecular level [7b]. In such arrangement, uniform morphology without any long-range phase separation was observed for the multilayer film and high IPCE (5.5%) and PCE (0.041 %) were obtained for 50 bilayer films.

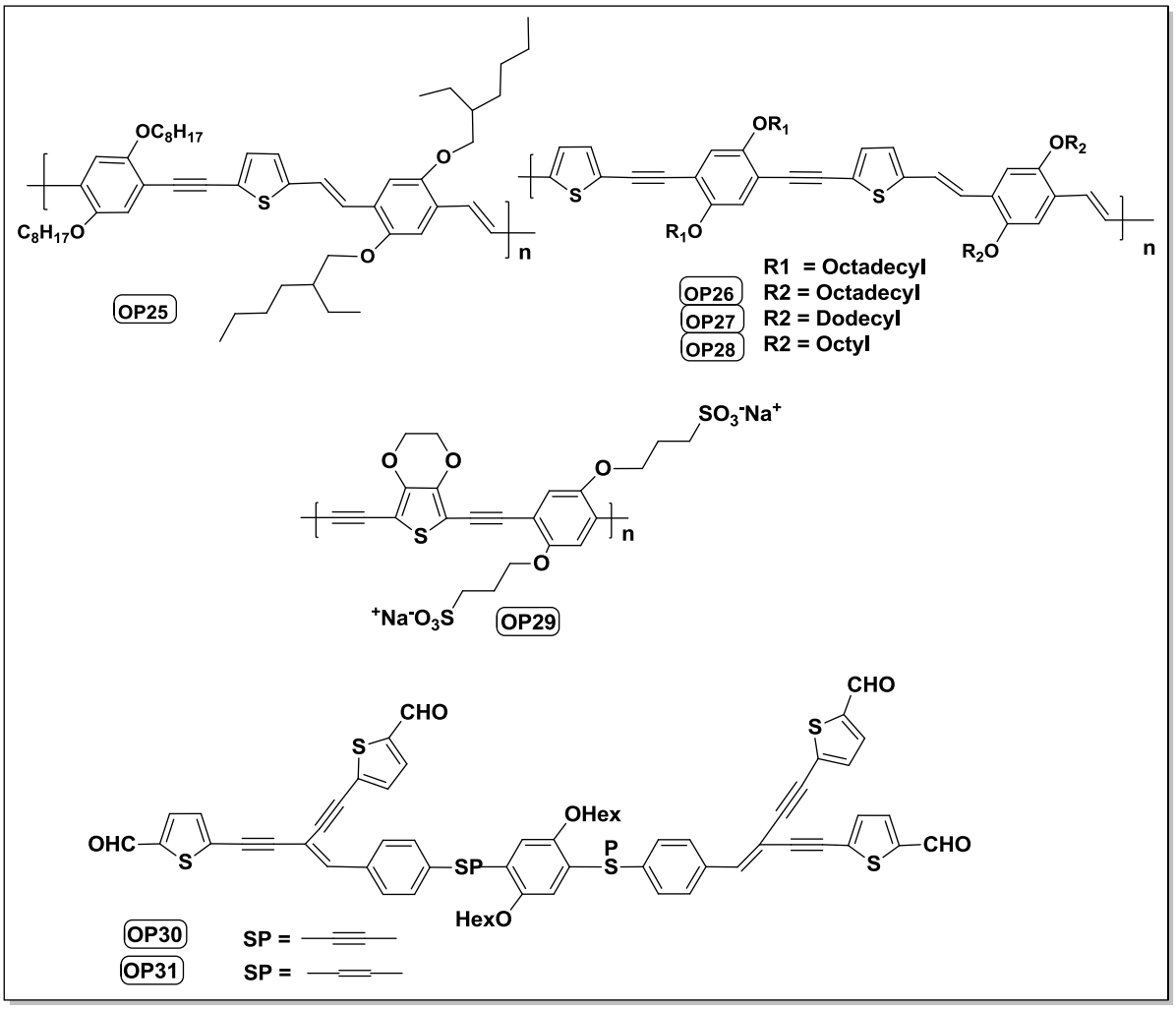

Chart 4: Oligo-ynes and poly-ynes incorporating hybrid spacers containing thiophene.

Fer et al. [76] synthesized the oligo-ynes **OP30-OP33** (**Chart 4** and **Chart 5**) but these exhibited only a modest performance with low FF (0.25 to 0.28) and V_{oc} (0.12 to 0.42 V) because of the low yield of long-lived triplet excited state. The J_{sc} of both **OP32** and **OP33** were low (< 1 mA/cm^2). The J_{sc} of **OP33** (J_{sc} = 0.27 mA/cm^2) was six times higher than that of **OP32** ascribed to the rapid charge recombination process. The better SC performance of **OP33** was favored by its extended absorption into the visible region and strong electron donating capacity. **OP31** showed high J_{sc} of 2.04 mA/cm^2 and better performance than that of **OP30**. The main reason for enhanced performance of **OP31** was its potential for generating free charge carriers, which were facilitated by the large phase separation. However, in **OP31**, 60% to 70% of charge carriers undergo recombination. The low FF was possibly due to its low hole mobility and hence recombination.

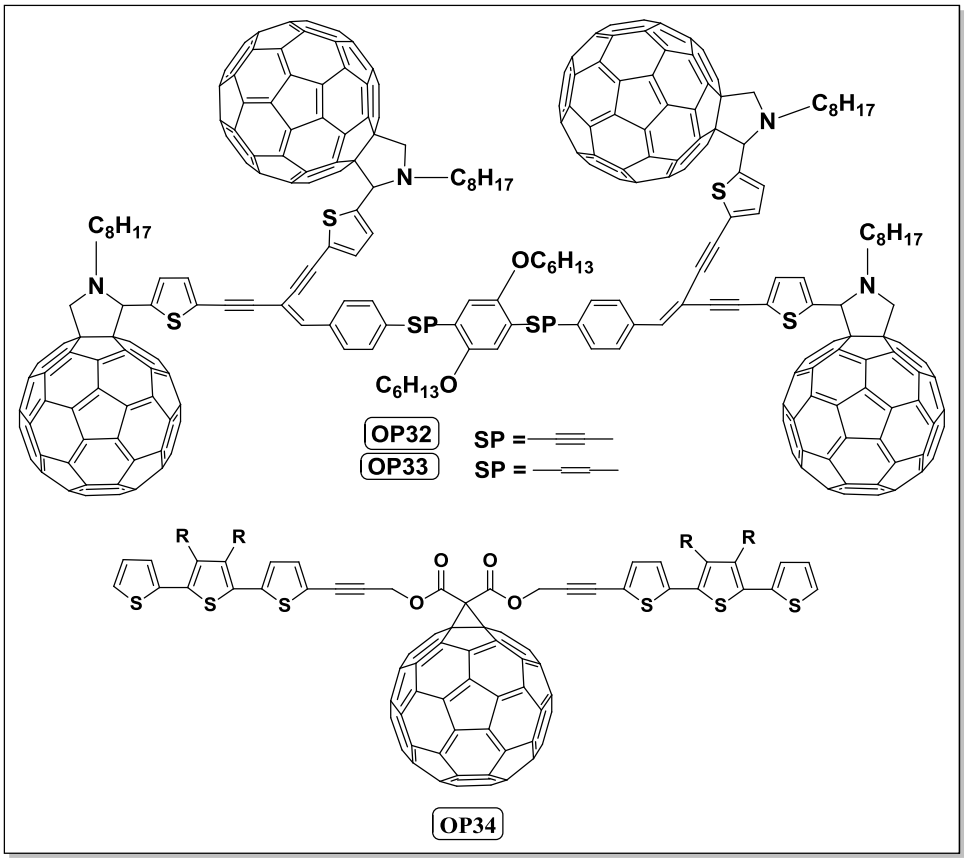

Chart 5: Thiophene containing di and oligo-ynes embedded with C_{60}.

Nisic et al. [77] reported **OP34** which has a high LUMO level with respect to PCBM, which improved the V_{oc}. The remarkably low-E_g (1.47 eV) of this material was also related to the high HOMO energy level. They confirmed the potential of **OP34** as an acceptor material from its red shifted absorption compared to that of PCBM. In **OP34** the LUMO energy level and hence E_g can be tuned by modifying the link between the fullerene and terthiophene.

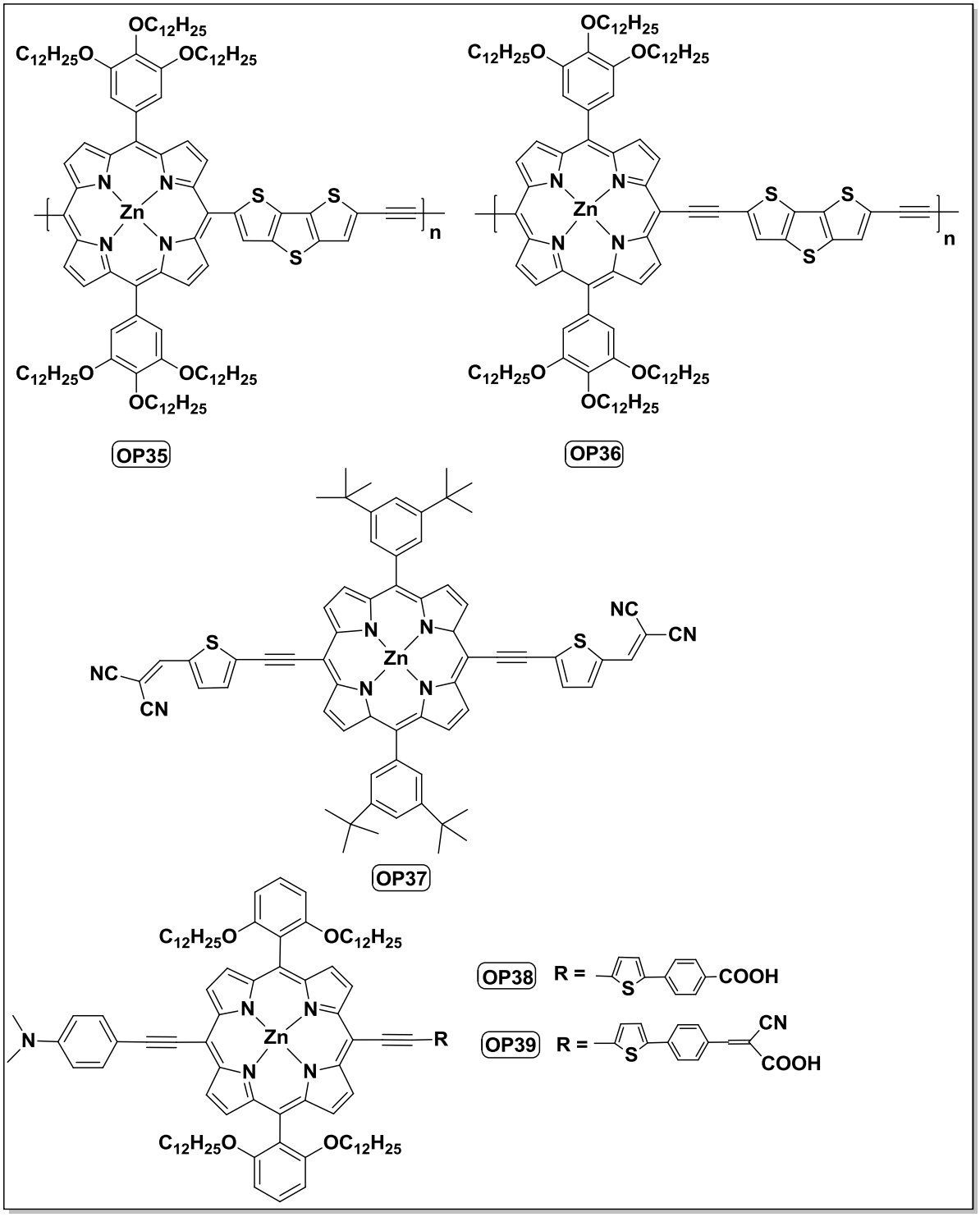

Chart 6: Porphyrin-based oligo-ynes incorporating thiophenes.

Macrocyclic systems such as porphyrin-based oligo-ynes are also good candidates for SCs owing to their better absorption profile. Several researchers have reported the efficacy of porphyrins and their analogs as active materials for SCs. Among them, Huang et al. [54b] reported porphyrin-based oligo-ynes **OP35** and **OP36 (Chart 6)**, in which the poly-yne with

C≡C bond (**OP36)** showed lower molecular weight and thermal stability than the single bond linked oligomer (**OP35)**. However, **OP36** showed higher mobility than that of **OP35** due to strong aggregation and intermolecular interaction in thin films, provided by the co-planarity of polymer. The **OP36**:PCBM (1:3, w/w) showed high PCE (0.3%) than that of **OP35**:PCBM (1:3, w/w), which was supported by the strong Q-band (a weak transition from the ground state to the first excited state) absorption (760 nm) and higher mobility (2.1×10^{-4} cm^2 $V^{-1}s^{-1}$) in **OP36**.

More recently, Kumar et al. [16b] synthesized the low-E_g (~ 1.58 eV), A-π-D-π-A based oligo-yne **OP37** which displayed a broad and intense absorption in the Vis-NIR region. The extended π-conjugation provided by the ethynylene link caused the dicyanovinyl substituted thiophene moiety to become coplanar to the porphyrin core. The high PCE of 3.65% and 5.24% shown by **OP37** depends on the solvent, THF and pyridine-THF, respectively. The better balanced charge transport was observed for the device with improved nano morphology of **OP37**:$PC_{71}BM$ active layer, which was processed by the pyridine-THF solvent. The device processed with pyridine-THF showed lower ratios of electron to hole mobility than that of THF processed device, leading to balanced charge transport. The high V_{oc} of THF processed SC device was attributed to the deeper HOMO energy level. Though there was different absorption for oligo-ynes based on the processing solvent, the similarity of IPCE in both the Soret and Q-band implied the same PCE.

Lu et al. [21a] synthesized the D-π-A based oligo-yne systems **OP38-OP39** as sensitizer materials for mesoscopic SC and demonstrated red shifted absorptions with various linker units. The PCE of 7.75% and 6.09% were shown by **OP38** and **OP39** dyes, respectively. The strong and directional electron excitation processes were facilitated by the D-π-A unit. The solubility and reduction in dye aggregation were improved by the presence of the 1,3-bis(dodecyloxy)-phenyl group, which led to reduction of interfacial charge recombination. The intra-molecular charge transfer was improved by the presence of the thiophene group and the rigid molecular structure was facilitated by the insertion of arene group. The replacement of benzoic acid by the cyanoacetic acid in the **OP39** dye led to the fast interfacial charge recombination. The charge extraction measurements showed faster interfacial charge recombination of photo-injected electrons with oxidized species of redox couple at the TiO_2/electrolyte interface in **OP39** (V_{oc} = 0.76 V) device compared to that of

OP38 (V_{oc} = 0.81 V), which was responsible for the drop in photo-voltage (about 50 mV) and photocurrent.

The performance parameters of the organic oligo-ynes and poly-ynes incorporating thiophene-based spacers are compiled in **Table 1**. The performance of the materials depends on various factors such as the type of hybrid spacers in the polymer backbone, the length of the polymer chain, the solubility of the materials, solvent, morphology and device architectures. Since thiophene-based spacers provide a good platform to tune the PV properties, it would be of advantage to further modify the structure of the thiophene-based spacers and evaluate the SC performances of the new poly-yne materials.

Table 1: SC performance parameters of some organic oligo-ynes and poly-ynes incorporating thiophene-based spacers.

Polymer	**Band gap (E_g, eV)**	**V_{oc} (V)**	**J_{sc} (mA/cm^2)**	**FF**	**PCE (%)**	**Ref.**
OP1	1.92	0.61	10.6	0.67	4.40	[68]
OP2	2.06	1.01	3.10	0.36	1.13	
OP3	1.76	0.84	4.8	0.37	1.5	[69]
OP4	1.86	0.88	4.4	0.35	1.3	
OP5	1.86	0.87	3.6	0.31	1.0	
OP6	1.97	0.94	4.2	0.40	1.6	
OP7	2.17	0.89	2.90	0.21	0.56	[55b]
OP8	2.24	0.67	0.47	0.33	0.13	
OP9	1.90	0.74	0.69	0.27	0.14	[19b]
OP10	2.14	0.93	7.04	0.44	2.87	[20]
OP11	2.06	0.94	7.24	0.48	3.28	
OP12	2.13	0.96	5.96	0.44	2.51	
OP13	1.99	0.85	6.45	0.43	2.36	
OP14	1.57	0.82	4.11	0.40	1.34	[55a]
OP15	1.53	0.74	5.87	0.40	1.74	
OP16	1.73	0.72	4.97	0.39	1.40	
OP17	1.60	-	-	-	-	[12c]
OP18	1.57	0.67	10.72	0.33	2.37	
OP19	1.57	0.70	4.45	0.43	1.36	

OP20	2.25	0.93	1.95	0.40	0.74	[26]
OP21	2.21	0.88	2.75	0.38	0.92	
OP22	2.25	0.82	1.45	0.37	0.43	
OP23	2.08	0.92	2.38	0.39	0.85	[74]
OP24	2.04	0.90	5.95	0.45	2.40	
OP25	2.10	0.90	2.51	0.54	1.21	[25, 75]
OP26	-	-	-	-	-	
OP27	2.10	0.50	1.44	0.37	0.27	
OP28	-	-	-	-	-	
OP29	-	0.26	0.50	0.31	0.041	[7b]
OP30	-	0.12	0.10	0.25	0.003	[76]
OP31	-	0.40	2.04	0.26	0.214	
OP32	-	0.42	0.04	0.28	0.005	
OP33	-	0.21	0.27	0.25	0.015	
OP34	1.47	-	-	-	-	[77]
OP35	4.8	0.45	0.45	0.29	0.06	[54b]
OP36	-	0.58	1.52	0.34	0.30	
OP37 (THF)	~ 1.58	0.94	8.82	0.44	3.65	[16b]
OP37 (THF-Pyridine)	~ 1.58	0.88	10.64	0.56	5.24	
OP38	-	0.81	12.66	0.75	7.75	[21a]
OP39	-	0.76	10.66	0.74	6.09	

4.2 Conjugated poly(metalla-ynes)

The inclusion of transition metals along the poly-yne chain not only extends the conjugation, but also augments the OE properties including the PCE of the polymeric materials [78]. This is because of the easy access to triplet states facilitated by the presence of heavy metal ions such as Pt(II), a contribution which is almost ineffective in the organic poly-ynes. In platina-ynes, the d-orbital of platinum (d_{xy} and d_{xz}) metal overlaps with alkyne p-orbitals (p_y* and p_z*) and enhances the π-electron delocalization along the polymer chain [79]. The relatively

long life-time of the triplet excited state enhances the probability of exciton diffusion to the D-A interface.

4.2.1 Pt(II)-based Poly-ynes

Since the demonstration by Köhler et al. [8a] of Pt(II) poly-ynes as active materials in SCs, a vast amount of research has been published using different spacers and metal ions, notably Pt(II) **(Chart 7)**. The inclusion of Pt(II) into the conjugated system enhances the interchain charge transport and populates the triplet excited state [80]. Furthermore, Pt(II) poly-ynes possess good solubility and hence better solution processability than organic poly-ynes [14]. Guo et al. [81] fabricated a SC device from a phosphorescent Pt(II) poly-yne containing thiophene, as the spacer group, and suggested that there was a contribution from the triplet excited state of the blend film in PET for PCEs. The excited state (spin-triplet) that precedes PET in BHJ shows the high capability of generating long-lived charge separated states. The SC device based on the 1:4 blend film of **MP1**:PCBM with 42 nm thickness displayed PCE of ~ 0.27% (V_{oc} = 0.64 V). There was a small drop in the PCEs and FF with increasing thickness of blend film, which was caused by the increase in the series resistance of the photoactive layer [82]. In the case of IPCE, the increase in PCE was observed with a concomitant decrease in photoactive layer thickness. Only ~ 22% of internal quantum efficiency was shown by the 42 nm thickness of the thin film as it absorbs only 40% of light at 400 nm. The PET was favorable from the polymer triplet state to PCBM as these were separated by a sufficiently large energy gap between ^{3}**MP1*** and the charge separated state (Fig. 4).

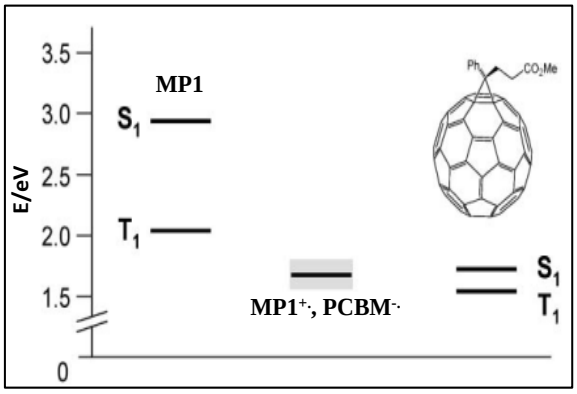

Fig. 4. Energy level diagram of **MP1** and PCBM (Reproduced with permission from Ref. [81])

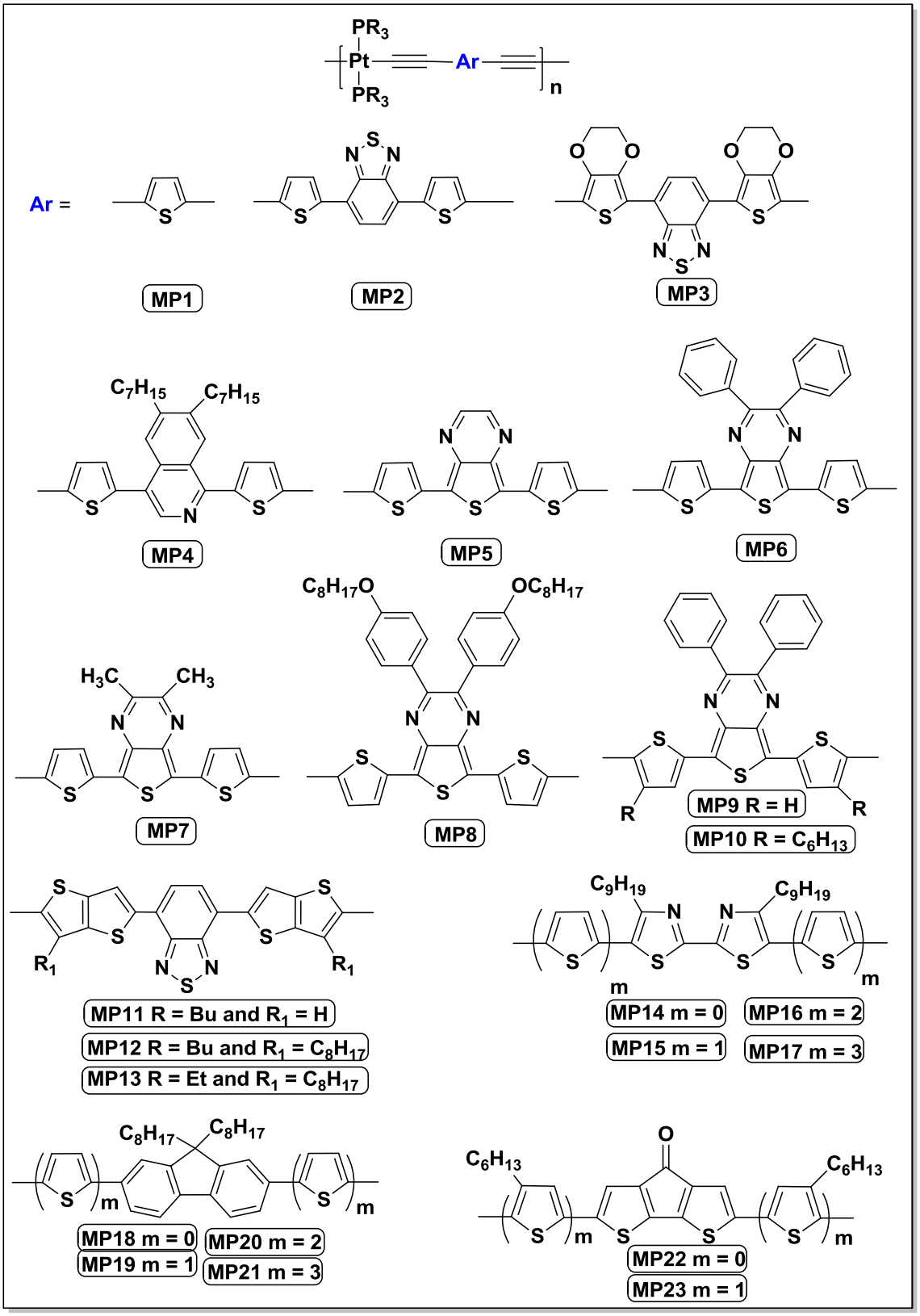

Chart 7: Chemical structures of poly(platina-ynes)

Wong et al. [10] reported an intensely colored low-E_g (1.85 eV) Pt(II) poly-yne **MP2** incorporating thiophene-BTD-thiophene hybrid spacers. Because of the better phase separation, the best SC performance (PCE = 4.93%) was obtained with a 1:4 ratio of blend film with J_{sc} = 15.43 mA/cm^2, V_{oc} = 0.82 V and FF = 0.39. The lower HOMO level of **MP2** (-5.3 eV) might be the reason for the high V_{oc} compared to that of SC device based on **OP1**/PCBM (HOMO = -5.20 eV), which showed PCE of only 1.61% (V_{oc} = 0.74 V, J_{sc} = 6.22 mA/cm^2 and FF = 0.35). Similarly, EQE of 87% was shown by **MP2**, which was higher than that observed for the **OP1**/PCBM based device (EQE = 67%). Additionally, a more balanced electron and hole transport was observed in **MP2**:PCBM blends. Low FF of the device was attributed to the space-charge limited performance [83]. Due to the enhanced absorption of the **MP2**:PCBM-based device, it was suggested that, for high PCE, the improvement of the absorption co-efficient of the polymer should also be considered besides the low-E_g. When the thiophene unit in **MP2** was replaced by EDOT, it resulted in strong visible light absorption and low-E_g polymer **MP3** [84]. The reduction in E_g compared to **MP2** was mainly due to the enhanced D-A interaction, which was further increased by the extensive delocalization in the conjugated polymer backbone **(**Fig. 5a**)**. The HOMO energy level of **MP3** was increased and hence the E_g of the material was reduced by the strong donor nature of the EDOT moieties. It was observed that the singlet state was mainly responsible for the charge generation in the SC material and not the triplet state due to the thermodynamic feasibility of charge transfer from singlet state [81]. **MP3**:PCBM showed low PCE of 0.78% compared to **MP2** (Fig. 5b). Decrease in J_{sc} with increase in thickness was attributed to low hole mobility and poor charge collection. Furthermore, the SC device processed with toluene showed a small increase in performance compared to the chlorobenzene processed analogue [21c].

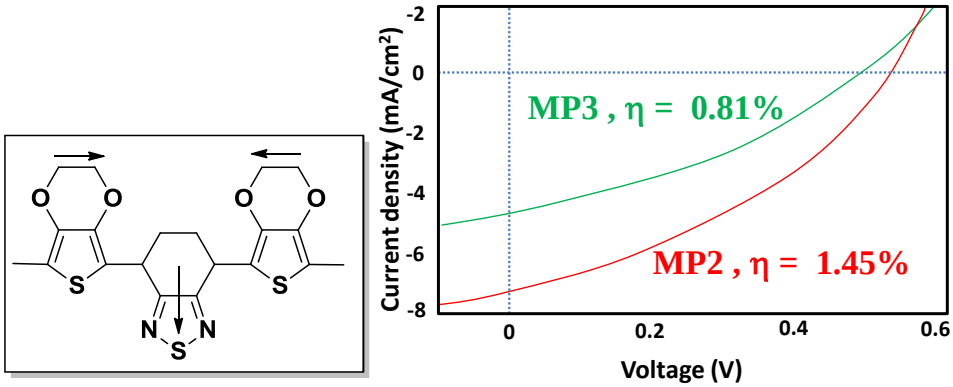

(a) (b)

Fig. 5. (a) Direction of electron transfer after excitation in poly(platina-yne) **MP3** [21c], (b) J-V characteristics of **MP2**:PCBM and **MP3**:PCBM under AM 1.5 simulated solar irradiation (Reproduced with permission from Ref. [84].

When the spacer was replaced by substituted quinoline and thienopyrazine units, a range of D-A systems were observed. Pei-Tzu et al. [12a] reported a series of low-E_g (1.49 to 1.97 eV) Pt(II) poly-ynes **(MP4-MP7)** for SC applications. On changing the spacer from **MP2** and **MP4** to strong acceptor units in **MP6** and **MP7**, an increase in ICT strength was observed. In the case of hole mobility, the polymers **MP2** and **MP7** showed higher average mobility than the others (**MP4-MP6)**, attributed to the low molecular weight [85]. The SC device based on **MP4-MP7** with $PC_{71}BM$ showed V_{oc} in the range of 0.39-0.66 V. The low value of V_{oc} of **MP6** (0.39 V) was attributed to low molecular weights, ionization potential and poor p-channel semiconducting behavior. **MP4-MP7** showed very low J_{sc} values ranging from 0.25 to 2.99 mA/cm^2 compared to **MP2**, which was the major limiting factor in this work. The very low value of FF ranging from 0.17-0.34 was shown by all Pt(II) poly-ynes, which may be due to their poor charge separation and charge transport. Wang et al. [21b] reported Pt(II) poly-yne **MP8** which was very similar to **MP6**, containing two additional octyloxy groups on the arene ring of pyrazine unit. Polymers with such a configuration gave E_g of 1.5 eV, PCE of 0.42% and EQE of 29.54 % with coverage of both NIR and visible region. Prior to this work, the same group [86] reported similar Pt(II) poly-ynes **MP9** and **MP10** having alkylated thiophenes. These solution processable, intensely colored low-E_g (1.47–1.50 eV) Pt(II) poly-yne also possessed strong D–A interactions. The PCE of 0.37% and 0.56% were achieved for **MP9** and **MP10**, respectively, with a blend ratio of 1:5. It was suggested that the FF could be improved by lowering the thickness of the active layer, which might also lower J_{sc} and PCE. When thiophene was replaced by substituted thienothiophene around the BTD unit (**MP11-MP13**), Pt(II) poly-ynes having E_g between 1.81-1.85 eV were obtained. Interestingly, these Pt(II) poly-ynes gave a very high PCE in the range of 2.63-4.13% [4b]. Among these polymers **MP11** showed higher hole mobility compared to **MP2**. This observation clearly explained the enhancement of electron coupling between D and A units along the polymer backbone by the incorporation of a more rigid structure [87]. **MP12** showed PCE of 3.76% with high J_{sc} and FF, 8.67 mA/cm^2 and 0.51, respectively. The hole mobility of **MP13** marginally increased by decreasing side chain length of the phosphine ligand (PEt_3), leading to decreased steric hindrance between two adjacent alkyl side chains.

The **MP13** material showed the best SC performance due to its high hole mobility (PCE = 4.13%). **MP13**:$PC_{71}BM$ showed enhanced PCE as it possessed large phase separation compared to a relatively smooth surface morphology.

Wong et al. [17f] reported strong visible light absorbing Pt(II) poly-ynes with thiadiazole as the acceptor (**MP14-MP17)**. The low-E_g polymer was found to possess a structure similar to the inorganic n-i-p-i based super lattice quantum well structure. Although **MP17** displayed an increased absorption at longer wavelength, both **MP16** and **MP15** when blended with PCBM showed carrier mobilities in the order of 10^{-4} $cm^2V^{-1}s^{-1}$ and similar PCEs. The changes in film roughness and phase separation in **MP16**:PCBM and **MP17**:PCBM blends were the cause for this observed trend [88]. **MP16** and **MP17** gave high PCE (2.14% and 2.50%, respectively). **MP17** showed strong absorption characteristics at longer wavelength compared to that of other Pt(II) poly-ynes with fewer thienyl rings **(MP14-MP16)**. **MP17**:PCBM showed slightly high PCE because of higher refractive index, which facilitated more reflection of light at the **MP17**:PCBM interface than that of **MP16**:PCBM. When the spacer in **MP14-MP17** was changed to a fluorene ring [23] (**MP18-MP21)**, a similar trend was observed. **MP18** and **MP19** showed lower mobility compared to **MP20** and **MP21**. Thus, changes in the number of thiophene rings along the polymeric chain not only tuned the optical properties, but also the charge transport properties [89]. PCEs of 2.11% and 2.41% were obtained for **MP20** and **MP21**, respectively. The dependence of EQE wavelength for the SC based on **MP2**:PCBM (1:4) and **MP18-MP21**/PCBM (1:5) are shown in Fig. 6 [19a]. The PCE rose sharply on going from **MP18** → **MP21** (i.e., **MP18** < **MP19** < **MP20** < **MP21**) at the blend ratio of 1:5. The high charge carrier mobility and good absorption characteristics were responsible for the high PCE of **MP21**. Though the E_g of the polymer was not very low (Eg > 2.3 eV), the high PCE of 2.41% clearly explained the significance of extending the overlap to achieve a polymer with broad absorption range in the visible spectrum with retention of high absorption co-efficient at appropriate wavelength. In addition, the suitable energy level of the polymer for interaction with PCBM could also be achieved by this approach. Wang et al. [17a] synthesized thermally and air stable bithiophene-based, low-E_g (1.44–1.53 eV) Pt(II) poly-ynes (**MP22** and **MP23)**. As expected, E_g was lowered with an increase in the number of thienyl rings and an increase in absorption was mainly caused by the effective π-conjugation [90] of C=O group with the dithiophene in **MP22** and tetrathiophene in **MP23**. The improved stability and PCE of 0.74% were shown

by **MP23** in the 1:4 blend ratio of Pt(II) poly-yne and PCBM respectively, compared to PCE of 0.34% in **MP22**. Recently, two new Pt(II) polymers containing diketopyrrolopyrrole and isoindigo spacers embedded between thiophene units **(MP24 and MP25, Chart 8**) have been reported by Wong et al. [91] These dark blue polymers look promising for SC applications as they show excellent absorption in visible region ($\lambda_{max.}$ = 664 and 678 nm) and have very low-E_g (1.58-1.70 eV).

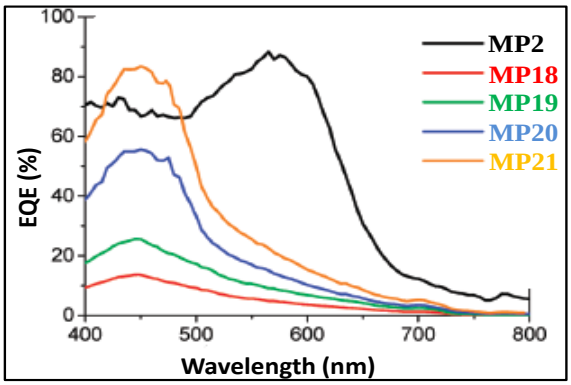

Fig. 6: The variation of EQE for the poly(platina-yne) **MP2** and **MP18**-**MP21** (Reproduced with permission from Ref. [19a]).

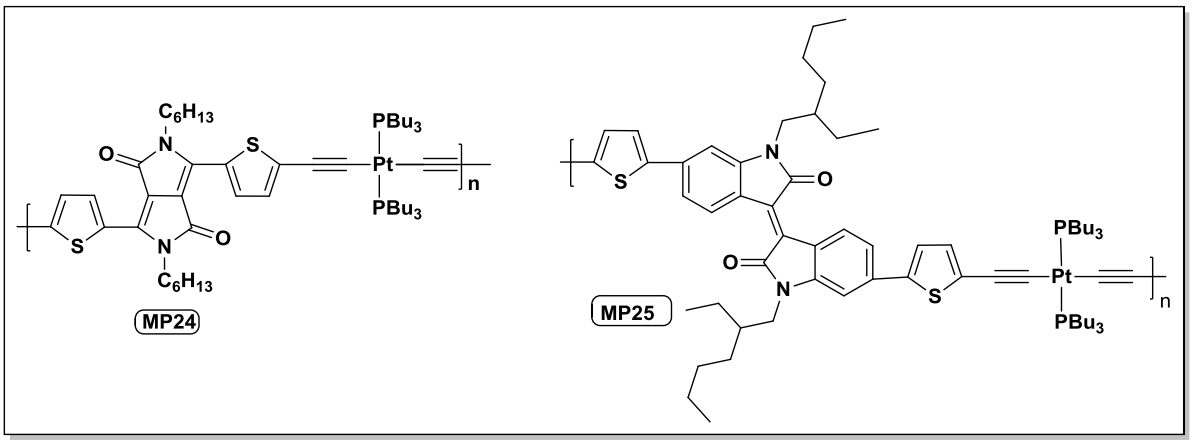

Chart 8: Pt(II) polymers containing diketopyrrolopyrrole and isoindigo spacers embedded between thiophene units.

Platinum(II) poly-ynes containing alternate electron-rich phenothiazine and thiophene (**MP26-MP28, Chart 9**) showed PCE ranging from 1.03% to 1.27% and exhibited linear dependence on the inverse of the oligothienyl chain length on the E_g [92]. Interestingly, these polymers do not show any phosphorescence which was ascribed to the presence of hetero-aryl rings which reduced the effects of Pt(II). Thus, the singlet excited state was mainly responsible for the efficient photo-induced charge separation. **MP28** showed higher

absorption and thus higher PCE than **MP27** due to the larger number of thienyl rings in **MP28**. Moreover, the electron and hole mobilities were enhanced when the number of thienyl ring was increased. The maximum EQE of 64.2 % (1:5 blend ratio) and 68.92% (1:4 blend ratio) was achieved for **MP27** and **MP28**, respectively. The low FF was caused by the poor phase separation at the D-A blend ratio.

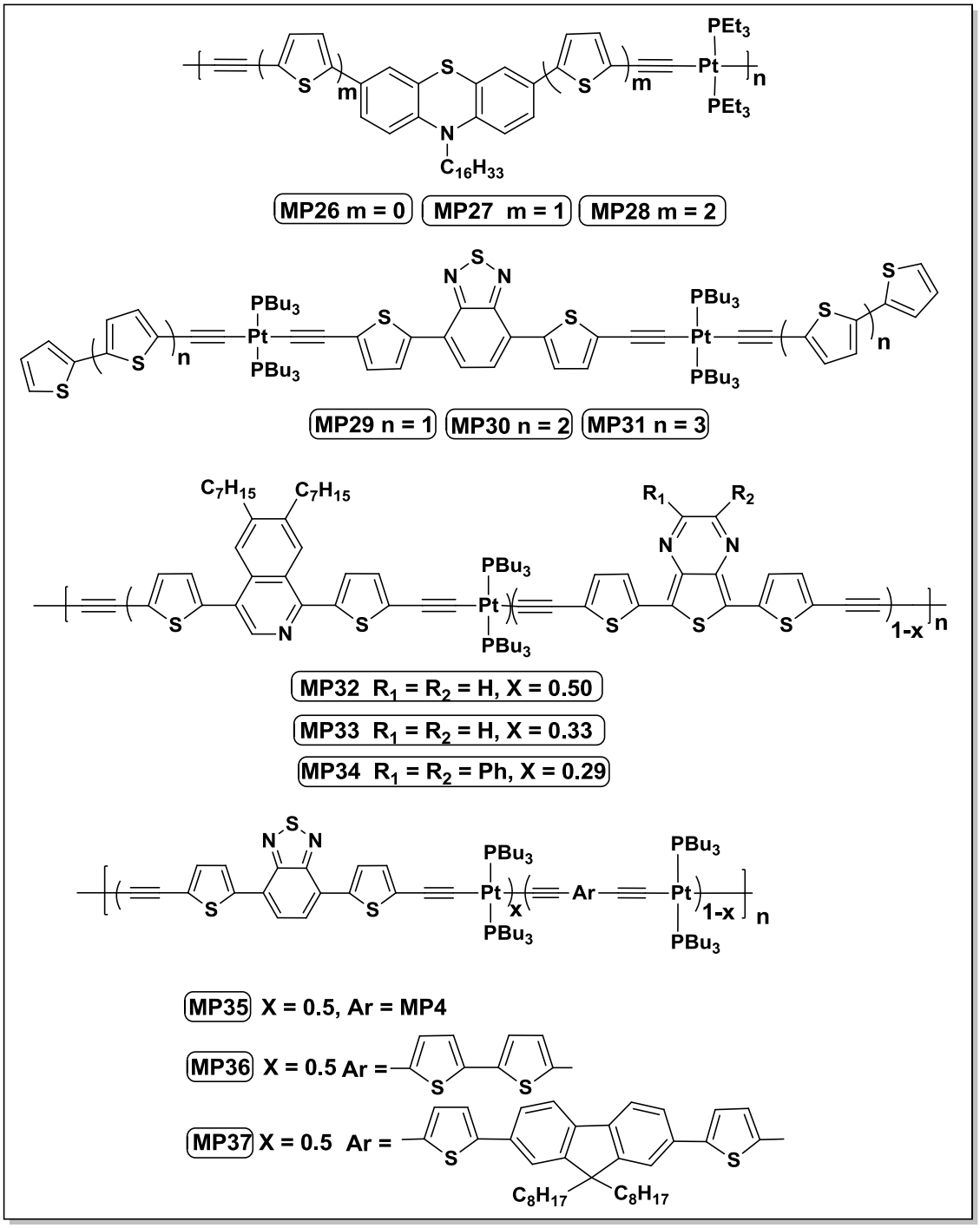

Chart 9: Pt(II) poly-ynes and oligo-ynes incorporating alternate D and A spacers.

Contrarily, oligo-ynes **MP29-MP31** containing BTD as the acceptor and central core, a thiophene ring as the termini and Pt(II) embedded between them possessed an E_g of 1.9 eV, and a PCE ranging from 2.2-3.0% [4c]. Tributylphospine (PBu_3) auxiliary ligands on the Pt(II) prevented aggregation of the polymers and offered good solution processability. However, increasing the oligothiophene length significantly shifted the absorption to the red; however, little effect was seen on the hole mobility. The Pt(II) poly-ynes **MP29-MP31** displayed a similar V_{oc}, ranging from 0.71 to 0.82 V. Among all the polymers, **MP30** exhibited the best SC performances at a 1:4 blend ratio of **MP30**:$PC_{71}BM$ with a PCE of 3.0% (J_{sc} = -8.45 mA/cm^2).

When co-polymers containing thienopyrazine and quinoline (**MP32-MP34**) were assessed, they gave a PCE in the range of 0.009-0.16% [12a]. The E_g of the Pt(II) poly-ynes was in the range of 1.53-1.55 eV. For these polymers, PCE and J_{sc} were found to increase in the following order **MP34 < MP33 < MP32**. However, **MP32** and **MP33** showed same V_{oc} (0.5 V) and FF (0.23) while **MP34** showed a lower FF (0.18). **MP37** showed a high PCE of 0.71% compared to **MP35** and **MP36.** Poor charge separation and charge transport properties of the polymer caused very low values of FF ranging from 0.20-0.25.

The SC based on poly-yne materials having fullerene units showed efficient charge separation and good PV response in pure solid materials. Guo et al. [93] reported fullerene end capped Pt(II) acetylide D-A triad **MP38** (**Chart 10**). It showed a PCE of 0.056% with J_{sc} of 0.5 mA/cm^2. The singlet and triplet state of Pt(II) acetylide chromophore were found to be strongly quenched in the triad assembly. The excited state quenching was increased due to intra-molecular PET from Pt(II) acetylide (D) to the fulleropyrrolidine (A).

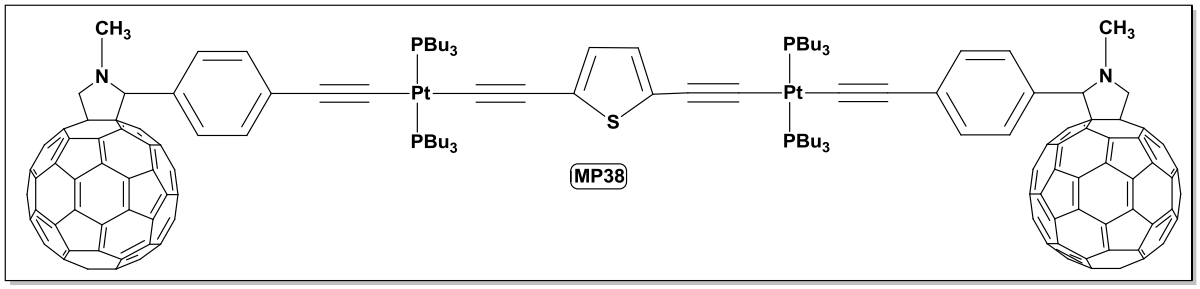

Chart 10: Fullerene end capped Pt(II) acetylide D-A triad.[93]

Wang et al. [22a] synthesized a new series of soluble thiophene-triarylamine based soluble Pt(II) poly-ynes having "*pseudo 3D*" dimensionality (**MP39-MP41, Chart 11**), which showed PCE in the range of 0.83-1.78%. The polymers exhibited high E_g (2.59 to 2.72

eV) due to the absence of D-A structure in the polymeric chain. However, they possessed extended π-electron delocalization through the triarylamine-thiophene segment and the electron-rich Pt(II). Enhancement in the absorption co-efficient was observed with increase in the dimensionality of the polymers. These 3D polymers displayed double absorptions and hence a 2-4 times higher PCE compared to that of the linear polymer. This effect was attributed to the better absorption and high charge transport properties of randomly oriented conjugated segments in the 3D multidimensional polymer than that of vertically oriented chains of the linear system. The difference in dimensionality of the structures also caused the higher V_{oc} of the **MP41**:PCBM compared to that of **MP39** or **MP40**:PCBM. However, imbalanced charge transport caused low FF (0.38-0.53). The enhanced absorption was observed in the range of 350-415 nm upon blending with 83% PCBM. The polymers **MP39** and **MP40** displayed the highest EQE values of 50.2% at 418 nm and 80.9% at 412 nm, respectively. The multi-dimensional polymer showed a higher surface roughness than that of the linear polymer because of significant phase establishment of larger PCBM domains and high reflection of light.

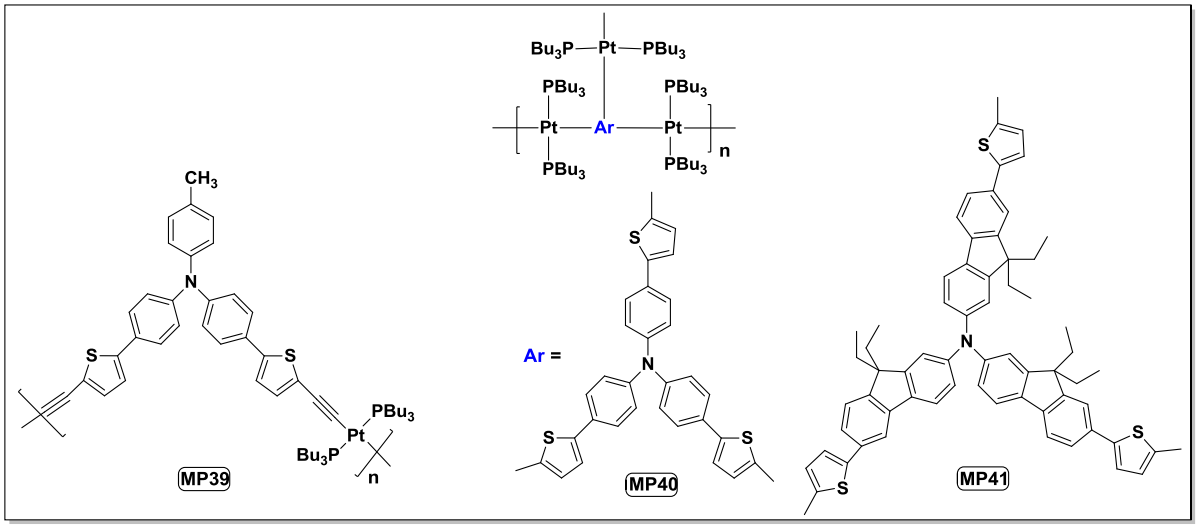

Chart 11: Thiophene-triarylamine based soluble Pt(II) poly-ynes.

Yuan et al. [94] achieved reduction in the polymer energy level by the cycloaddition–retro-electrocyclization reaction of main chain alkynes of Pt(II) poly-ynes containing D-A-D units with tetracyanoethylene (TCNE) **MP42-MP44** (**Chart 12**). When TCNE was added to the Pt(II) poly-yne, the LUMO levels were significantly reduced and consequently the absorption moved to longer wavelength. However, a weak photocurrent was observed when **OP1** and TCNE-adducted polymers were mixed. A clear photo-current generation was

observed when **MP42** was mixed with PCBM. **MP42**-based SC devices displayed low PCE compared to that for **MP2**. The SC fabricated with **MP43**-**MP44** also showed lower PCEs, which was probably due to the reduced carrier mobility by the TCNE addition [95] and, subsequently, caused noticeable decrease in the J_{sc} values. In addition, lack of nanoscale phase separation also caused low J_{SC} for **MP43** and **MP44**-based devices. Improvements in both J_{sc} and FF were observed when PCBM was replaced by $PC_{71}BM$, which was attributed to significant features of $PC_{71}BM$ such as extended absorption and inhibition of charge recombination. The SC device based on **OP1** and **MP43** showed a PCE of 0.00079%. The device fabricated from the combination of **OP1** and **MP44** did not show any photocurrent under similar conditions. The poor SC performance of **MP44** compared to **MP43** was probably caused by the lower LUMO level of **MP44**.

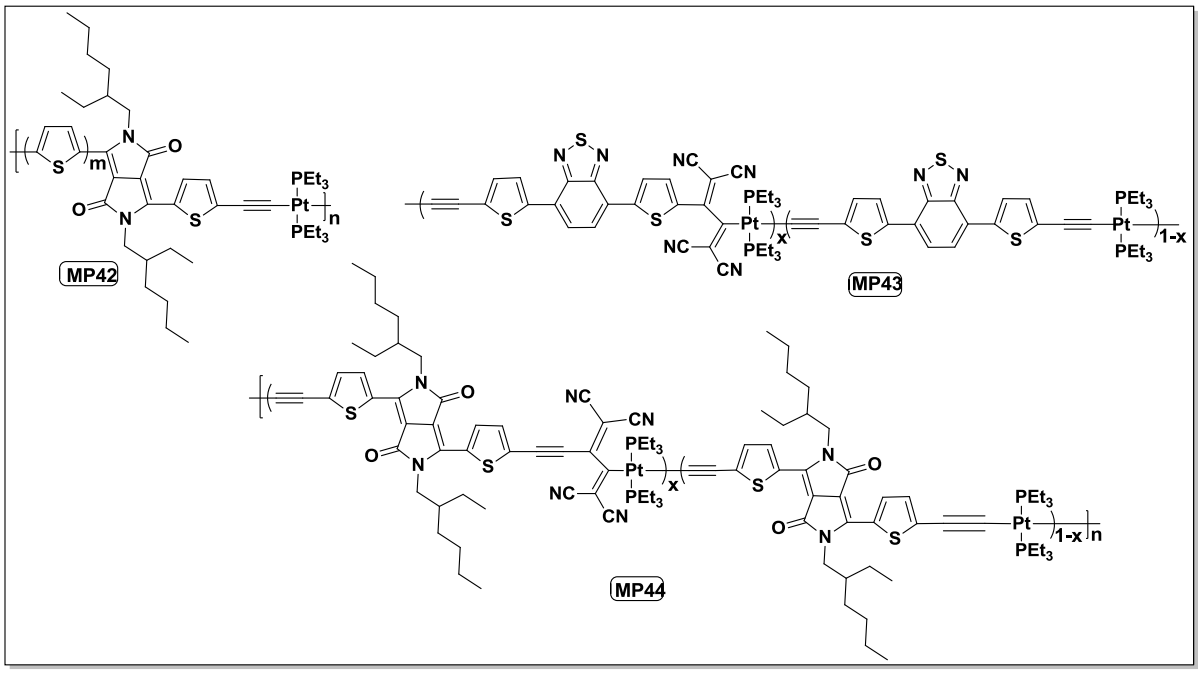

Chart 12: Pt(II) poly-ynes containing D-A-D units with tetracyanoethylene (TCNE).

Cui et al. [96] reported low-lying HOMO oligo-ynes **MP45-MP48** (**Chart 13**) in which the energy levels were similar to the LUMO of $PC_{70}BM$. The highest PCE of 1.59% (V_{oc} = 0.93 V) was shown by **MP46**:$PC_{70}BM$ (3:7), which exhibited a decrease in PCE (1.06%) with a change in the blend ratio to 1:4 (**MP46**:$PC_{70}BM$). A similar high PCE of 1.56% was also exhibited by the **MP48**:$PC_{70}BM$ at a 1:4 blend ratio. However, it decreased to 1.42% with a blend ratio of 3:7 (**MP48**:$PC_{70}BM$). **MP45**:PCBM showed PCE of 0.88%,

which decreased with increasing blend ratio. The poor SC performance (0.17%) was displayed by the **MP47**:$PC_{70}BM$ blend with no change in PCE on varying the blend ratio.

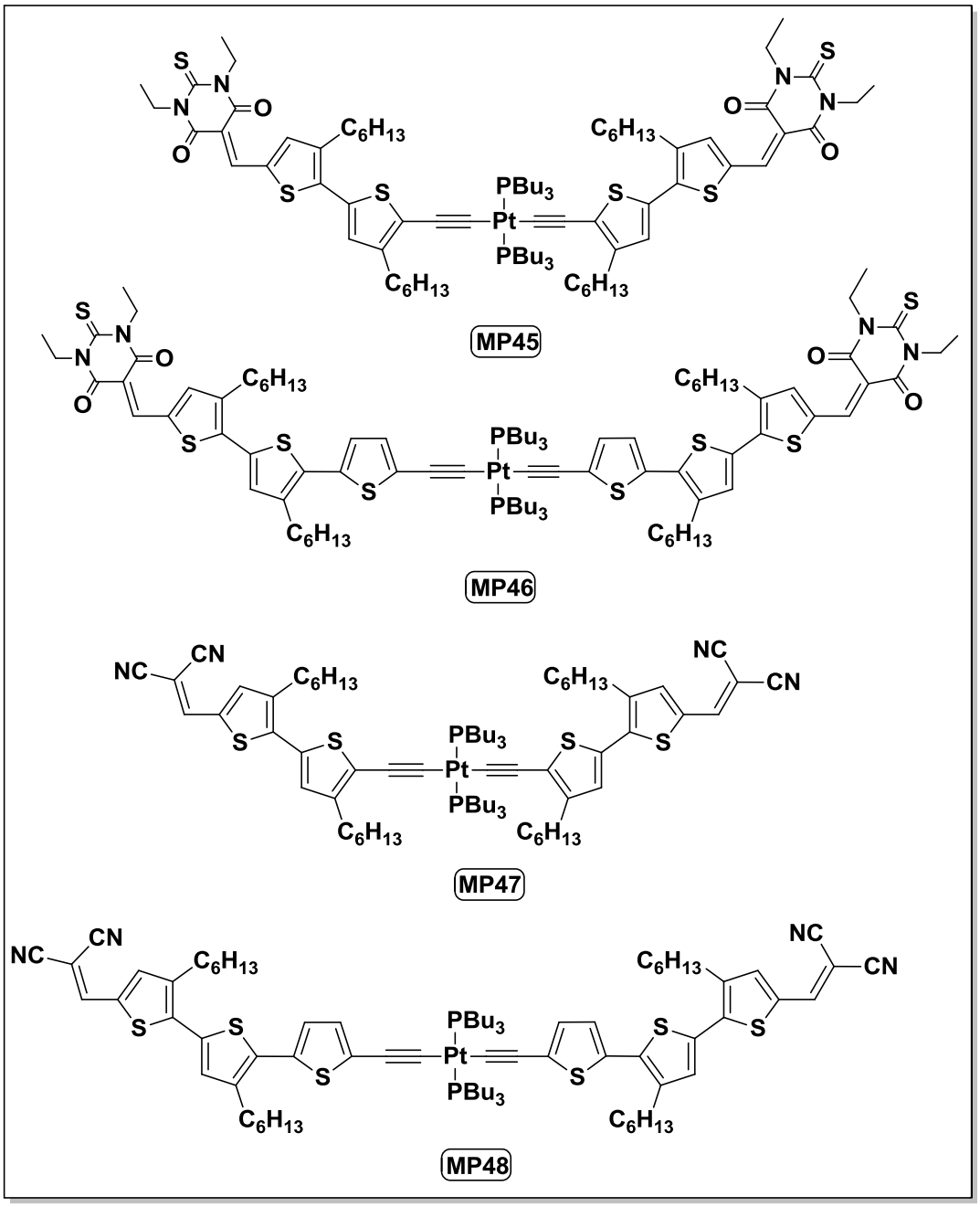

Chart 13: Low-lying HOMO oligo-ynes.

The SC parameters of oligo- and poly(platina-ynes) incorporating thiophene-based spacers are given in **Table 2**. The PCE values are somewhat lower than those of the organic counterparts, but the role of metal ion in extending electron delocalization along the polymer backbone and modifying the opto-electronic properties is very well known. Moreover, trialkylphosphine (PR_3) ligands impart better physical properties (*viz.* enhanced solubility,

reduced aggregation etc) to the Pt(II) poly-ynes compared to their purely organic counterparts. Therefore, it is worthwhile investigating "*novel poly(platina-ynes)*" in the quest for developing novel metal-based donor materials for SC applications.

Table 2: SC performance parameters of some di- and poly(metalla-yne)s incorporating thiophene-based spacers.

Polymer	**Band gap (E_g, eV)**	**V_{oc} (V)**	**J_{sc} (mA/cm^2)**	**FF**	**PCE (%)**	**Ref.**
MP1	-	0.64	0.99	0.43	0.27	[81]
MP2	1.85	0.82	15.43	0.39	4.93	[10]
MP3	1.84	0.50	4.56	0.35	0.78	[84]
MP4	1.97	0.66	2.99	0.34	0.68	[12a]
MP5	1.54	0.52	2.71	0.26	0.36	
MP6	1.49	0.39	0.25	0.17	0.02	
MP7	1.66	0.53	2.14	0.28	0.32	
MP8	1.50	0.52	2.61	0.31	0.42	[21b]
MP9	1.50	0.55	2.04	0.34	0.37	[86]
MP10	1.47	0.50	2.90	0.38	0.56	
MP11	1.84	0.84	7.33	0.39	2.69	[4b]
MP12	1.82	0.81	8.67	0.51	3.76	
MP13	1.81	0.79	9.61	0.49	4.13	
MP14	2.46	0.73	0.91	0.32	0.21	[17f]
MP15	2.28	0.83	2.33	0.39	0.76	
MP16	2.22	0.81	6.93	0.38	2.14	
MP17	2.19	0.88	6.50	0.44	2.50	
MP18	2.93	0.74	1.22	0.37	0.33	[23]
MP19	2.60	0.95	2.50	0.58	1.36	
MP20	2.43	0.94	4.05	0.56	2.11	
MP21	2.33	0.89	6.59	0.41	2.41	
MP22	1.53	0.71	1.65	0.29	0.34	[17a]
MP23	1.44	0.68	3.15	0.34	0.74	

MP24	1.70	-	-	-	-	[91]
MP25	1.58	-	-	-	-	
MP26	-	-	-	-	-	[92]
MP27	2.66	0.76	3.70	0.37	1.03	
MP28	2.52	0.78	4.00	0.39	1.27	
MP29	1.9	0.71	-7.91	0.42	2.30	[4c]
MP30	1.9	0.82	-8.54	0.43	3.00	
MP31	1.9	0.73	-7.66	0.40	2.20	
MP32	1.55	0.50	1.39	0.23	0.16	[12a]
MP33	1.54	0.50	0.99	0.23	0.11	
MP34	1.53	0.32	0.17	0.18	0.009	
MP35	1.68	0.52	0.86	0.25	0.11	
MP36	1.89	0.64	2.35	0.20	0.31	
MP37	1.88	0.68	4.21	0.25	0.71	
MP38	-	0.41	0.50	0.28	0.056	[93]
MP39	2.72	0.74	2.99	0.38	0.83	[22a]
MP40	2.68	0.76	4.79	0.44	1.60	
MP41	2.59	0.82	4.09	0.53	1.78	
MP42	1.79	0.51	2.97	0.35	0.53	[94]
MP43	1.47	0.26	1.29	0.29	0.10	
MP44	1.28	0.59	0.68	0.27	0.09	
MP45	1.76	0.91	3.61	0.28	0.88	[96]
MP46	1.69	0.93	5.89	0.29	1.59	
MP47	1.88	0.60	1.22	0.34	0.17	
MP48	1.91	0.92	4.88	0.33	1.56	
MP49	1.66	0.40	0.66	0.31	0.10	[97]
MP50	-	0.43	1.5	0.47	0.30	[95]

4.2.2 Non Pt(II)-based Poly-ynes

The use of non Pt(II)-based oligo-ynes/poly-ynes as donor materials for polymer SC is limited, but it also seems to be a promising area of research. Recently, a Ru-based oligo-yne has been used as a sensitizer material for DSSC [95]. **MP49** (**Chart 14**) was the first Ru-

based oligo-yne, which was used as a photoactive donor for the BHJ SC. Colombo et al. [97] reported a low-E_g (1.66 eV), Ru-based oligo-yne **MP49**. The BHJ based on the blend of **MP49** and PCBM at 1:2 ratio showed V_{oc} = 0.4 V, FF = 0.31 and J_{sc} = 0.66 mA/cm^2. The low PCE (0.1%) of the device was due to the strong tendency to phase segregate between **MP49** and PCBM, which affected both photo-generation yields and charge transport to the electrodes. It was suggested that the photo absorption and transfer to PCBM by the oligo-yne was the main cause for the strong photocurrent enhancement. In addition, the red shift of the photocurrent spectral response was observed for the **MP49** compared to the SC device made from corresponding Pt(II)-based material [84], indicating the potential of Ru oligo-ynes as effective donors for SC applications. The energetics of charge separation from oligo-yne to PCBM hardly varied by the substitution of Pt by Ru [84]. Recently, Nisic et al. [95] reported a dipolar π-delocalized Ru(II) dialkynyl complex **MP50**. It also showed low PCE of 0.3 %, which was attributed to the unmatched energy levels between the dye and TiO_2. Low J_{sc} of 1.5 mA/cm^2 was shown by **MP50**, which indicated poor charge transfer process.

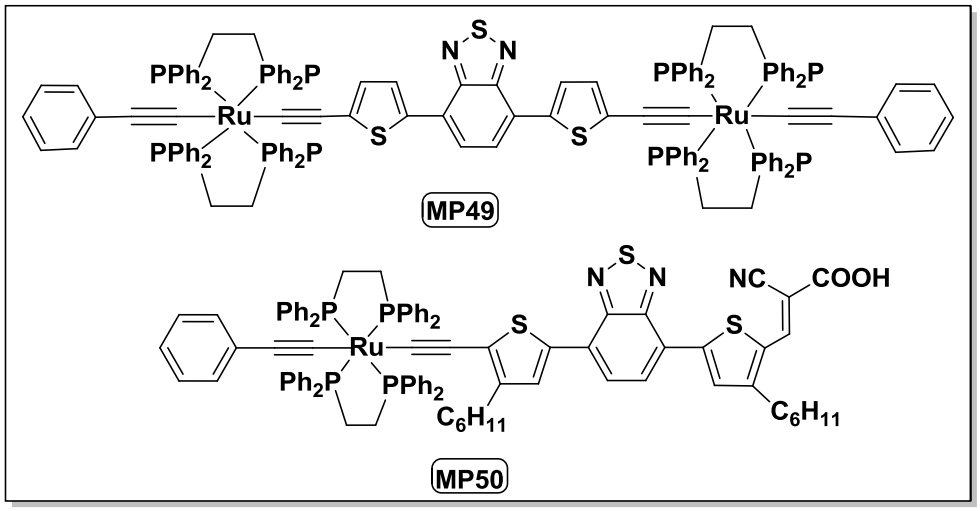

Chart 14: Ru-based oligo-yne used as a sensitizer material for DSSC.

5. Conclusions and Future directions

The exponential growth in global energy demands and the depletion of fossil fuels worldwide have created immense pressure on the scientific community working in the field of SCs. Silicon based SCs exhibit high PCE (26%) and are widely used to convert solar energy into electricity. Conjugated poly-yne and poly(metalla-yne) based SCs exhibit lower PCE but they have several advantages, e.g. light weight, low cost, solubility, processability, flexibility and tailoring of molecular structure. For commercial applications, novel poly-yne and

poly(metalla-yne) materials need to be developed with PCE above 10% [11a, 18a, 21a]. In order to achieve high PCE, polymers with low-E_g, high absorption (visible to NIR region), matching energy level with the acceptor (fullerene), high charge carrier mobility and excellent film forming ability are badly needed [69]. Several research groups have accomplished the synthesis of extremely narrow-E_g materials through the introduction of alternate D-A units in the polymer backbone. This approach enhances the extended π-electron delocalization and hence reduces the energy gap of the polymers, which results in extended absorption in the NIR region. In the case of organic poly-ynes, the energetic losses should be reduced to obtain high PCE, which can be achieved by making V_{oc} as high as possible. It is interesting to note that the introduction of the C≡C group enhances the V_{oc} of the polymer through raising its oxidation potential. Poly(metalla-ynes) have an advantage over organic poly-ynes in terms of solution processability. Thiophene-based donors in SC possess an added advantage in that the E_g of the polymer can be lowered by increasing the number of thienyl rings, leading to enhanced absorption and hence high PCE. The physical properties of the polymers can also be tuned by varying the substituents on the thiophene ring. Consequently, conjugated poly-ynes and poly(metalla-ynes) incorporating thiophene spacers are attracting considerable research interest in the context of solar energy conversion. Some remarkable progress in PCE has been achieved over the last two decades. The large volume of research reveals that the overall efficiency of SCs are strongly influenced by factors such as the type of spacers [4b, 20, 23], the position of C≡C bonds [69],the molecular weight [98], the charge carrier mobility [22a], the crystallinity [99], the thermal stability [100], the morphology [58d] and the device architecture [41]. We hope thiophene-incorporated poly-yne and poly(metalla-yne) materials will soon have a bright future in efficient solar energy conversion.

Acknowledgements

The literature review leading to this review paper was conducted with funding from The Research Council (TRC), Oman under the Open Research Grant No. ORG/SQU/EI/13/015. JM acknowledges the TRC for a PhD scholarship, AH acknowledges the TRC for a Postdoctoral fellowship and MSK acknowledges the Sultan Qaboos University, Oman for a research leave. PRR is grateful to the EPSRC for continued funding (EP/K004956/1).

References

[1] (a) I. Chapman, Energ. Policy 64 (2014) 93-101; (b) C. Sener, V. Fthenakis, Renew. Sust. Energ. Rev. 32 (2014) 854-868; (c) E. McFarland, Energy Environ. Sci. 7 (2014) 846-854.

[2] (a) Z. He, H. Wu, Y. Cao, Adv. Mater. 26 (2014) 1006-1024; (b) F.E. Ala'a, J.-P. Sun, I.G. Hill, G.C. Welch, J. Mater. Chem. A 2 (2014) 1201-1213.

[3] Fachlexikon der Physik, Verlag Harri Deutsch, 2. Auflage (1989)

[4] (a) P.-L.T. Boudreault, A. Najari, M. Leclerc, Chem. Mater. 23 (2010) 456-469; (b) N.S. Baek, S.K. Hau, H.-L. Yip, O. Acton, K.-S. Chen, A.K.-Y. Jen, Chem. Mater. 20 (2008) 5734-5736; (c) X. Zhao, C. Piliego, B. Kim, D.A. Poulsen, B. Ma, D.A. Unruh, J.M. Fréchet, Chem. Mater. 22 (2010) 2325-2332.

[5] (a) M. Grätzel, Inorg. Chem. 44 (2005) 6841-6851; (b) M. Grätzel, Acc. Chem. Res. 42 (2009) 1788-1798; (c) S. Mathew, A. Yella, P. Gao, R. Humphry-Baker, B.F. Curchod, N. Ashari-Astani, I. Tavernelli, U. Rothlisberger, M.K. Nazeeruddin, M. Grätzel, Nat. Chem. 6 (2014) 242-247; (d) G. Li, R. Zhu, Y. Yang, Nat. Photonics 6 (2012) 153-161; (e) Y. Li, Acc. Chem. Res. 45 (2012) 723-733; (f) C. Cui, W.-Y. Wong, Y. Li, Energy Environ. Sci. 7 (2014) 2276-2284; (g) C. Qin, Y. Fu, C.H. Chui, C.W. Kan, Z. Xie, L. Wang, W.Y. Wong, Macromol. Rapid Commun. 32 (2011) 1472-1477; (h) J. Xiang, C.-L. Ho, W.-Y. Wong, Polym. Chem. 10.1039/C5PY00941C (2015)

[6] K. Barnham, M. Mazzer, B. Clive, Nat. Mater. 5 (2006) 161-164.

[7] (a) G.R. Whittell, M.D. Hager, U.S. Schubert, I. Manners, Nat. Mater. 10 (2011) 176-188; (b) J.K. Mwaura, M.R. Pinto, D. Witker, N. Ananthakrishnan, K.S. Schanze, J.R. Reynolds, Langmuir 21 (2005) 10119-10126; (c) C.-L. Ho, W.-Y. Wong, Coord. Chem. Rev. 255 (2011) 2469-2502; (d) F. Silvestri, A. Marrocchi, Int. J. Mol. Sci. 11 (2010) 1471-1508.

[8] (a) A. Köhler, H.F. Wittmann, R.H. Friend, M.S. Khan, J. Lewis, Synth. Met. 67 (1994) 245-249; (b) A. Köhler, H.F. Wittmann, R.H. Friend, M.S. Khan, J. Lewis, Synth. Met. 77 (1996) 147-150.

[9] N. Tore, E.A. Parlak, T.A. Tumay, P. Kavak, Ş. Sarıoğlan, S. Bozar, S. Günes, C. Ulbricht, D.A.M. Egbe, J. Nanopart. Res. 16 (2014) 1-8.

[10] W.-Y. Wong, X.-Z. Wang, Z. He, A.B. Djurišić, C.-T. Yip, K.-Y. Cheung, H. Wang, C.S. Mak, W.-K. Chan, Nat. mater. 6 (2007) 521-527.

[11] (a) J. Peet, J. Kim, N.E. Coates, W.L. Ma, D. Moses, A.J. Heeger, G.C. Bazan, Nat. Mater. 6 (2007) 497-500; (b) J.C. Bijleveld, M. Shahid, J. Gilot, M.M. Wienk, R.A. Janssen, Adv. Funct. Mater. 19 (2009) 3262-3270.

[12] (a) P.-T. Wu, T. Bull, F.S. Kim, C.K. Luscombe, S.A. Jenekhe, Macromolecules 42 (2009) 671-681; (b) F. Zhang, W. Mammo, L.M. Andersson, S. Admassie, M.R. Andersson, O. Inganäs, Adv. Mater. 18 (2006) 2169-2173; (c) R.S. Ashraf, M. Shahid, E. Klemm, M. Al‐Ibrahim, S. Sensfuss, Macromol. Rapid Commun. 27 (2006) 1454-1459.

[13] S. Zhang, Y. Guo, H. Fan, Y. Liu, H.Y. Chen, G. Yang, X. Zhan, Y. Liu, Y. Li, Y. Yang, J. Polym. Sci., Part A: Polym. Chem. 47 (2009) 5498-5508.

[14] W.Y. Wong, Macromol. Chem. Phys. 209 (2008) 14-24.

[15] E. Zhou, S. Yamakawa, K. Tajima, C. Yang, K. Hashimoto, Chem. Mater. 21 (2009) 4055-4061.

[16] (a) Y. Yuan, T. Michinobu, Macromol. Chem. Phys. 213 (2012) 2114-2119; (b) K.C. Vijay, L. Cabau, E. Koukaras, G. Sharma, E. Palomares, Nanoscale 7 (2015) 179-189.
[17] (a) X.Z. Wang, Q. Wang, L. Yan, W.Y. Wong, K.Y. Cheung, A. Ng, A.B. Djurišić, W.K. Chan, Macromol. Rapid Commun. 31 (2010) 861-867; (b) Q. Zhou, Q. Hou, L. Zheng, X. Deng, G. Yu, Y. Cao, Appl. Phys. Lett. 84 (2004) 1653-1655; (c) M. Svensson, F. Zhang, S.C. Veenstra, W.J. Verhees, J.C. Hummelen, J.M. Kroon, O. Inganäs, M.R. Andersson, Adv. Mater. 15 (2003) 988-991; (d) M.C. Scharber, D. Mühlbacher, M. Koppe, P. Denk, C. Waldauf, A.J. Heeger, C.J. Brabec, Adv. Mater. 18 (2006) 789-794; (e) J.Y. Kim, S.H. Kim, H.H. Lee, K. Lee, W. Ma, X. Gong, A.J. Heeger, Adv. Mater. 18 (2006) 572-576; (f) W.-Y. Wong, X.-Z. Wang, Z. He, K.-K. Chan, A.B. Djurišic, K.-Y. Cheung, C.-T. Yip, A.M.-C. Ng, Y.Y. Xi, C.S. Mak, J. Am. Chem. Soc. 129 (2007) 14372-14380; (g) Y. Kim, S. Cook, S.M. Tuladhar, S.A. Choulis, J. Nelson, J.R. Durrant, D.D. Bradley, M. Giles, I. McCulloch, C.-S. Ha, Nat. Mater. 5 (2006) 197-203; (h) G. Li, V. Shrotriya, J. Huang, Y. Yao, T. Moriarty, K. Emery, Y. Yang, Nat. Mater. 4 (2005) 864-868; (i) O. Oklobia, T. Shafai, Sol. Energy Mater. Sol. Cells 122 (2014) 158-163.
[18] (a) A.S. Abd-El-Aziz, Macromol. Rapid Commun. 23 (2002) 995-1031; (b) B.J. Holliday, T.M. Swager, Chem. Commun. (2005) 23-36; (c) C.A. Fustin, P. Guillet, U.S. Schubert, J.F. Gohy, Adv. Mater. 19 (2007) 1665-1673; (d) F.R. Dai, H.M. Zhan, Q. Liu, Y.Y. Fu, J.H. Li, Q.W. Wang, Z. Xie, L. Wang, F. Yan, W.Y. Wong, Chem. Eur. J. 18 (2012) 1502-1511.
[19] (a) W.-Y. Wong, C.-L. Ho, Acc. Chem. Res. 43 (2010) 1246-1256; (b) Z. Wu, B. Fan, F. Xue, C. Adachi, J. Ouyang, Sol. Energy Mater. Sol. Cells 94 (2010) 2230-2237.
[20] H. Zhan, Q. Liu, F. Dai, C.L. Ho, Y. Fu, L. Li, L. Zhao, H. Li, Z. Xie, W.Y. Wong, Chem. Asian J. 10 (2015) 1017-1024.
[21] (a) J. Lu, B. Zhang, H. Yuan, X. Xu, K. Cao, J. Cui, S. Liu, Y. Shen, Y. Cheng, J. Xu, J. Phys. Chem. C 118 (2014) 14739-14748; (b) X.-Z. Wang, C.-L. Ho, L. Yan, X. Chen, X. Chen, K.-Y. Cheung, W.-Y. Wong, J. Inorg. Organomet. Polym. Mater. 20 (2010) 478-487; (c) W.-Y. Wong, X. Wang, H.-L. Zhang, K.-Y. Cheung, M.-K. Fung, A.B. Djurišić, W.-K. Chan, J. Organomet. Chem. 693 (2008) 3603-3612.
[22] (a) Q. Wang, Z. He, A. Wild, H. Wu, Y. Cao, U. S. Schubert, C.H. Chui, W.Y. Wong, Chem.–Asian J. 6 (2011) 1766-1777; (b) H. Zhan, S. Lamare, A. Ng, T. Kenny, H. Guernon, W.-K. Chan, A.B. Djurišić, P.D. Harvey, W.-Y. Wong, Macromolecules 44 (2011) 5155-5167.
[23] L. Liu, C.L. Ho, W.Y. Wong, K.Y. Cheung, M.K. Fung, W.T. Lam, A.B. Djurišić, W.K. Chan, Adv. Funct. Mater. 18 (2008) 2824-2833.
[24] B.C. Thompson, J.M. Fréchet, Angew. Chem. Int. Ed. 47 (2008) 58-77.
[25] D.A.M. Egbe, L. H. Nguyen, D. Mühlbacher, H. Hoppe, K. Schmidtke, N. S Sariciftci, Thin Solid Films 511 (2006) 486-488.
[26] G. Adam, T. Yohannes, M. White, A. Montaigne, C. Ulbricht, E. Birckner, S. Rathgeber, C. Kästner, H. Hoppe, N.S. Sariciftci, Macromol. Chem. Phys. 215 (2014) 1473-1484.
[27] (a) D.I.K. Petritsch, Organic Solar Cell Architectures, PhD Thesis, Technisch-Naturwissenschaftliche Fakult¨at der Technischen Universit¨at Graz (Austria) (2000) ; (b) T. Kirchartz, J. Bisquert, I. Mora-Sero, G. Garcia-Belmonte, Phys. Chem. Chem. Phys. 17 (2015) 4007-4014; (c) K.A. Mazzio, C.K. Luscombe, Chem. Soc. Rev. 44 (2015) 78-90; (d) T. Ameri, G. Dennler, C. Lungenschmied, C.J. Brabec, Energy Environ. Sci. 2 (2009) 347-363; (e) J. Roncali, Acc. Chem. Res. 42 (2009) 1719-1730.

[28] (a) H.-Y. Chen, J. Hou, S. Zhang, Y. Liang, G. Yang, Y. Yang, L. Yu, Y. Wu, G. Li, Nat. Photonics 3 (2009) 649-653; (b) Y. Liang, Z. Xu, J. Xia, S.T. Tsai, Y. Wu, G. Li, C. Ray, L. Yu, Adv. Mater. 22 (2010) E135-E138.
[29] H. Zeng, X. Zhu, Y. Liang, X. Guo, Polymers 7 (2015) 333-372.
[30] (a) Q. Xu, T. Song, W. Cui, l. yuqiang, W. Xu, S.-T. Lee, B. Sun, Appl. Mater. Interfaces (2015) 10.1021/am508006q; (b) A. Savva, E. Georgiou, G. Papazoglou, A.Z. Chrusou, K. Kapnisis, S.A. Choulis, Sol. Energy Mater. Sol. Cells 132 (2015) 507-514; (c) S. Xiao, L. Chen, L. Tan, L. Huang, F. Wu, Y. Chen, J. Phys. Chem. C 119 (2015) 1943-1952.
[31] H.-L. Yip, A.K.-Y. Jen, Energy Environ. Sci. 5 (2012) 5994-6011.
[32] (a) J. Huang, G. Li, Y. Yang, Adv. Mater. 20 (2008) 415-419; (b) H.-H. Liao, L.-M. Chen, Z. Xu, G. Li, Y. Yang, Appl. Phys. Lett. 92 (2008) 173303; (c) G. Li, C.-W. Chu, V. Shrotriya, J. Huang, Y. Yang, Appl. Phys. Lett. 88 (2006) 253503.
[33] (a) C. Waldauf, M. Morana, P. Denk, P. Schilinsky, K. Coakley, S. Choulis, C. Brabec, Appl. Phys. Lett. 89 (2006) 233517; (b) H. Hänsel, H. Zettl, G. Krausch, R. Kisselev, M. Thelakkat, H.W. Schmidt, Adv. Mater. 15 (2003) 2056-2060; (c) J.K. Lee, N.E. Coates, S. Cho, N.S. Cho, D. Moses, G.C. Bazan, K. Lee, A.J. Heeger, Appl. Phys. Lett. 92 (2008) 243308.
[34] M.H. Park, J.H. Li, A. Kumar, G. Li, Y. Yang, Adv. Funct. Mater. 19 (2009) 1241-1246.
[35] (a) M. White, D. Olson, S. Shaheen, N. Kopidakis, D.S. Ginley, Appl. Phys. Lett. 89 (2006) 143517; (b) R. Zhou, Y. Zheng, L. Qian, Y. Yang, P.H. Holloway, J. Xue, Nanoscale 4 (2012) 3507-3514; (c) L. Qian, J. Yang, R. Zhou, A. Tang, Y. Zheng, T.-K. Tseng, D. Bera, J. Xue, P.H. Holloway, J. Mater. Chem. 21 (2011) 3814-3817; (d) I. Gonzalez-Valls, M. Lira-Cantu, Energy Environ. Sci. 2 (2009) 19-34.
[36] S.K. Hau, H.-L. Yip, N.S. Baek, J. Zou, K. O'Malley, A.K.-Y. Jen, Appl. Phys. Lett. 92 (2008) 253301.
[37] (a) Y. Sun, W. Zhang, H. Chi, Y. Liu, C.L. Hou, D. Fang, Renew. Sust. Energ. Rev 43 (2015) 973-980; (b) T. Hu, L. Chen, Z. Deng, Y. Chen, J. Mater. Chem. A 3 (2015) 10890-10899; (c) A. Morais, J.P.C. Alves, F.A.S. Lima, M. Lira-Cantu, A.F. Nogueira, J. Photon. Energy 5 (2015) 057408.
[38] M. Wang, Q. Tang, J. An, F. Xie, J. Chen, S. Zheng, K.Y. Wong, Q. Miao, J. Xu, Appl. Mater. Interfaces 2 (2010) 2699-2702.
[39] D. Gao, M.G. Helander, Z.B. Wang, D.P. Puzzo, M.T. Greiner, Z.H. Lu, Adv. Mater. 22 (2010) 5404-5408.
[40] M. Wang, F. Xie, W. Xie, S. Zheng, N. Ke, J. Chen, N. Zhao, J. Xu, Appl. Phys. Lett. 98 (2011) 183304.
[41] W. Cao, J. Xue, Energy Environ. Sci. 7 (2014) 2123-2144.
[42] H. Jun, M. Careem, A. Arof, Renew. Sust. Energ. Rev. 22 (2013) 148-167.
[43] P. Baruch, A. De Vos, P. Landsberg, J. Parrott, Sol. Energy Mater. Sol. Cells 36 (1995) 201-222.
[44] (a) S. Besold, U. Hoyer, J. Bachmann, T. Swonke, P. Schilinsky, R. Steim, C. Brabec, Sol. Energy Mater. Sol. Cells 124 (2014) 133-137; (b) L. Slooff, S. Veenstra, J. Kroon, W. Verhees, L. Koster, Y. Galagan, Phys. Chem. Chem. Phys. 16 (2014) 5732-5738.
[45] M.A. Green, Solid State Electron. 24 (1981) 788-789.
[46] S. Günes, N.S. Sariciftci, Inorg. Chim. Acta 361 (2008) 581-588.
[47] (a) S. Günes, H. Neugebauer, N.S. Sariciftci, Chem. Rev. 107 (2007) 1324-1338; (b) J.-M. Nunzi, C. R. Physique 3 (2002) 523-542; (c) http://plasticphotovoltaics.org/lc/lc-polymersolarcells/lc-how.html. (Last accessed on 31st May 2015)

[48] B.A. Gregg, J. Phys. Chem. B 107 (2003) 4688-4698.
[49] B.A. Gregg, M.C. Hanna, J. Appl. Phys. 93 (2003) 3605-3614.
[50] (a) H. Sirringhaus, P.J. Brown, R.H. Friend, M.M. Nielsen, K. Bechgaard, B.M.W. Langeveld-Voss, A.J.H. Spiering, R.A.J. Janssen, E.W. Meijer, P. Herwig, D.M. de Leeuw, Nature 401 (1999) 685-688; (b) H. Fell, E. Samuelsen, J. Als-Nielsen, G. Grübel, J. Mårdalen, Solid State Commun. 94 (1995) 843-846; (c) K. Yamamoto, S. Ochiai, X. Wang, Y. Uchida, K. Kojima, A. Ohashi, T. Mizutani, Thin Solid Films 516 (2008) 2695-2699.
[51] P. Heremans, D. Cheyns, B.P. Rand, Acc. Chem. Res. 42 (2009) 1740-1747.
[52] (a) F. Baert, C. Cabanetos, A. Leliège, E. Kirchner, O. Segut, O. Alévêque, M. Allain, G. Seo, S. Jung, D. Tondelier, J. Mater. Chem. C 3 (2015) 390-398; (b) V. Malytskyi, J.-J. Simon, L. Patrone, J.-M. Raimundo, RSC Adv. 5 (2015) 354-397; (c) T.T.T. Bui, M. Jahandar, C.E. Song, Q.V. Hoang, J.-C. Lee, S.K. Lee, I.-N. Kang, S.-J. Moon, W.S. Shin, Sol. Energy Mater. Sol. Cells 134 (2015) 148-156.
[53] (a) J.-S. Wu, S.-W. Cheng, Y.-J. Cheng, C.-S. Hsu, Chem. Soc. Rev. (2015) ; (b) P. Zhou, D. Dang, J. Fan, W. Xiong, C. Yang, H. Tan, Y. Wang, Y. Liu, W. Zhu, Dyes Pigment 112 (2015) 99-104; (c) M.S. Khan, M.K. Al-Suti, H.H. Shah, S. Al-Humaimi, F.R. Al-Battashi, J.K. Bjernemose, L. Male, P.R. Raithby, N. Zhang, A. Köhler, Dalton Trans. 40 (2011) 10174-10183.
[54] (a) F. Wudl, M. Kobayashi, A. Heeger, J. Org. Chem. 49 (1984) 3382-3384; (b) X. Huang, C. Zhu, S. Zhang, W. Li, Y. Guo, X. Zhan, Y. Liu, Z. Bo, Macromolecules 41 (2008) 6895-6902.
[55] (a) R.S. Ashraf, J. Gilot, R.A. Janssen, Sol. Energy Mater. Sol. Cells 94 (2010) 1759-1766; (b) F. Silvestri, A. Marrocchi, M. Seri, C. Kim, T.J. Marks, A. Facchetti, A. Taticchi, J. Am. Chem. Soc. 132 (2010) 6108-6123.
[56] (a) P. Kubis, L. Lucera, F. Machui, G. Spyropoulos, J. Cordero, A. Frey, J. Kaschta, M.M. Voigt, G.J. Matt, E. Zeira, Org. Electron. 15 (2014) 2256-2263; (b) T.M. Burke, M.D. McGehee, Adv. Mater. 26 (2014) 1923-1928; (c) D. Chi, S. Qu, Z. Wang, J. Wang, J. Mater. Chem. C 2 (2014) 4383-4387.
[57] (a) Y. Wei, Y. Yang, J.-M. Yeh, Chem. Mater. 8 (1996) 2659-2666; (b) J.-P. Lère-Porte, J.J. Moreau, C. Torreilles, Eur. J. Org. Chem. 2001 (2001) 1249-1258.
[58] (a) R.D. McCullough, Adv. Mater. 10 (1998) 93-116; (b) H.E. Katz, Z. Bao, S.L. Gilat, Acc. Chem. Res. 34 (2001) 359-369; (c) A. Mishra, C.-Q. Ma, P. Bäuerle, Chem. Rev. 109 (2009) 1141-1276; (d) M.T. Dang, L. Hirsch, G. Wantz, J.D. Wuest, Chem. Rev. 113 (2013) 3734-3765.
[59] (a) A. Yokoyama, R. Miyakoshi, T. Yokozawa, Macromolecules 37 (2004) 1169-1171; (b) S. Savagatrup, A.D. Printz, D. Rodriquez, D.J. Lipomi, Macromolecules 47 (2014) 1981-1992; (c) R.D. McCullough, R.D. Lowe, J. Chem. Soc. Chem. Commun. (1992) 70-72.
[60] (a) Y.-J. Cheng, S.-H. Yang, C.-S. Hsu, Chem. Rev. 109 (2009) 5868-5923; (b) D. R -Borja, J.-L. Maldonado, O. B -García, M. Rodríguez, E. P -Gutiérrez, R. F -Ramírez, G. de la Rosa, Synth. Met. 200 (2015) 91-98; (c) A. Vojtko, M. Benkovicova, Y. Halahovets, M. Jergel, M. Kotlar, M. Kaiser, P. Siffalovic, V. Nadazdy, E. Majkova, *P3HT:PCBM Based Organic Solar Cells: Structure Optimization and Improving External Quantum Efficiency by Plasmonic Nanoparticles Incorporation*, in *Nano-Structures for Optics and Photonics*, 2015; (d) S. Karuthedath, T. Sauermann, H.-J. Egelhaaf, R. Wannemacher, C.J. Brabec, L. Lüer, J. Mater. Chem. A 3 (2015) 3399-3408.

[61] V. Shrotriya, J. Ouyang, R.J. Tseng, G. Li, Y. Yang, Chem. Phys. Lett. 411 (2005) 138-143.
[62] M.-Y. Chiu, U.-S. Jeng, M.-S. Su, K.-H. Wei, Macromolecules 43 (2009) 428-432.
[63] E. von Hauff, J. Parisi, V. Dyakonov, Thin Solid Films 511 (2006) 506-511.
[64] (a) Y. Zhao, G. Yuan, P. Roche, M. Leclerc, Polymer 36 (1995) 2211-2214; (b) X. Yang, J. Loos, S.C. Veenstra, W.J. Verhees, M.M. Wienk, J.M. Kroon, M.A. Michels, R.A. Janssen, Nano Lett. 5 (2005) 579-583.
[65] (a) F. Padinger, R.S. Rittberger, N.S. Sariciftci, Adv. Funct. Mater. 13 (2003) 85-88; (b) D.A.M. Egbe, T. Kietzke, B. Carbonnier, D. Mühlbacher, H.-H. Hörhold, D. Neher, T. Pakula, Macromolecules 37 (2004) 8863-8873; (c) W. Ma, C. Yang, X. Gong, K. Lee, A.J. Heeger, Adv. Funct. Mater. 15 (2005) 1617-1622.
[66] C.H. Woo, B.C. Thompson, B.J. Kim, M.F. Toney, J.M. Fréchet, J. Am. Chem. Soc. 130 (2008) 16324-16329.
[67] Y. Zhao, S. Shao, Z. Xie, Y. Geng, L. Wang, J. Phys. Chem. C 113 (2009) 17235-17239.
[68] J. Cremer, P. Bäuerle, M.M. Wienk, R.A. Janssen, Chem. Mater. 18 (2006) 5832-5834.
[69] C. Du, W. Li, C. Li, Z. Bo, J. Polym. Sci. Part A: Polym. Chem. 51 (2013) 383-393.
[70] A.S. Özen, C. Atilgan, G. Sonmez, J. Phys. Chem. C 111 (2007) 16362-16371.
[71] Y. Yamashita, K. Ono, M. Tomura, S. Tanaka, Tetrahedron 53 (1997) 10169-10178.
[72] P. Sonar, S.P. Singh, S. Sudhakar, A. Dodabalapur, A. Sellinger, Chem. Mater. 20 (2008) 3184-3190.
[73] W. Yue, Y. Zhao, S. Shao, H. Tian, Z. Xie, Y. Geng, F. Wang, J. Mater. Chem. 19 (2009) 2199-2206.
[74] S. Wen, X. Bao, W. Shen, C. Gu, Z. Du, L. Han, D. Zhu, R. Yang, J. Polym. Sci., Part A: Polym. Chem. 52 (2014) 208-215.
[75] D.A.M. Egbe, B. Carbonnier, D. Mühlbacher, N.S. Sariciftci, Polymer 46 (2005) 9585-9595.
[76] G. Fernández, L. Sánchez, D. Veldman, M.M. Wienk, C. Atienza, D.M. Guldi, R.A. Janssen, N. Martín, J. Org. Chem. 73 (2008) 3189-3196.
[77] F. Nisic, A. Colombo, C. Dragonetti, A. Cominetti, A. Pellegrino, N. Perin, R. Po, A. Tacca, Int. J. Photoenergy Article ID 373497 (2014) doi:10.1155/2014/373497.
[78] (a) M.D. McGehee, Nat. Photonics 3 (2009) 250-252; (b) S.H. Park, A. Roy, S. Beaupre, S. Cho, N. Coates, J.S. Moon, D. Moses, M. Leclerc, K. Lee, A.J. Heeger, Nat. Photonics 3 (2009) 297-302.
[79] (a) H. Masai, K. Sonogashira, N. Hagihara, Bull. Chem. Soc. Jpn. 44 (1971) 2226-2230; (b) M.S. Khan, M.R. Al-Mandhary, M.K. Al-Suti, B. Ahrens, M.F. Mahon, L. Male, P.R. Raithby, C.E. Boothby, A. Köhler, Dalton Trans. (2003) 74-84.
[80] (a) Y. Liu, S. Jiang, K. Glusac, D.H. Powell, D.F. Anderson, K.S. Schanze, J. Am. Chem. Soc. 124 (2002) 12412-12413; (b) C.-L. Ho, W.-Y. Wong, Coord. Chem. Rev. 257 (2013) 1614-1649.
[81] F. Guo, Y.-G. Kim, J.R. Reynolds, K.S. Schanze, Chem. Commun. (2006) 1887-1889.
[82] M. Wolf, H. Rauschenbach, Adv. Energy Conv. 3 (1963) 455-479.
[83] (a) V.D. Mihailetchi, H. Xie, B. de Boer, L.J.A. Koster, P.W. Blom, Adv. Funct. Mater. 16 (2006) 699-708; (b) V.D. Mihailetchi, L.J.A. Koster, P.W. Blom, C. Melzer, B. de Boer, J.K. van Duren, R.A. Janssen, Adv. Funct. Mater. 15 (2005) 795-801.
[84] J. Mei, K. Ogawa, Y.-G. Kim, N.C. Heston, D.J. Arenas, Z. Nasrollahi, T.D. McCarley, D.B. Tanner, J.R. Reynolds, K.S. Schanze, Appl. Mater. Interfaces 1 (2009) 150-161.

[85] R.J. Kline, M.D. McGehee, E.N. Kadnikova, J. Liu, J.M. Frechet, M.F. Toney, Macromolecules 38 (2005) 3312-3319.
[86] X.-Z. Wang, W.-Y. Wong, K.-Y. Cheung, M.-K. Fung, A.B. Djurišić, W.-K. Chan, Dalton Trans. (2008) 5484-5494.
[87] F.C. Grozema, C. Houarner-Rassin, P. Prins, L.D. Siebbeles, H.L. Anderson, J. Am. Chem. Soc. 129 (2007) 13370-13371.
[88] X. Zhan, Z.a. Tan, B. Domercq, Z. An, X. Zhang, S. Barlow, Y. Li, D. Zhu, B. Kippelen, S.R. Marder, J. Am. Chem. Soc. 129 (2007) 7246-7247.
[89] N. Chawdhury, A. Köhler, R. Friend, W.-Y. Wong, J. Lewis, M. Younus, P. R. Raithby, T. Corcoran, M. Al-Mandhary, M. Khan, J. Chem. Phys. 110 (1999) 4963-4970.
[90] Q. Wang, W.-Y. Wong, Polym. Chem. 2 (2011) 432-440.
[91] Q. Liu, C.-L. Ho, Y. Lo, H. Li, W.-Y. Wong, J. Inorg. Organomet. Polym. Mater. 25 (2015) 159-168.
[92] W.-Y. Wong, W.-C. Chow, K.-Y. Cheung, M.-K. Fung, A.B. Djurišić, W.-K. Chan, J. Organomet. Chem. 694 (2009) 2717-2726.
[93] F. Guo, K. Ogawa, Y.-G. Kim, E.O. Danilov, F.N. Castellano, J.R. Reynolds, K.S. Schanze, Phys. Chem. Chem. Phys. 9 (2007) 2724-2734.
[94] Y. Yuan, T. Michinobu, J. Oguma, T. Kato, K. Miyake, Macromol. Chem. Phys. 214 (2013) 1465-1472.
[95] F. Nisic, A. Colombo, C. Dragonetti, E. Garoni, D. Marinotto, S. Righetto, F. De Angelis, M.G. Lobello, P. Salvatori, P. Biagini, Organometallics 34 (2015) 94-104.
[96] C. Cui, Y. Zhang, W.C. Choy, H. Li, W.-Y. Wong, Science China Chem. 58 (2015) 347-356.
[97] A. Colombo, C. Dragonetti, D. Roberto, R. Ugo, L. Falciola, S. Luzzati, D. Kotowski, Organometallics 30 (2011) 1279-1282.
[98] R.J. Kline, M.D. McGehee, M.F. Toney, Nat. Mat. 5 (2006) 222-228.
[99] W. Ma, J.Y. Kim, K. Lee, A.J. Heeger, Macromol. Rapid Commun. 28 (2007) 1776-1780.
[100](a) M. Jørgensen, K. Norrman, S.A. Gevorgyan, T. Tromholt, B. Andreasen, F.C. Krebs, Adv. Mater. 24 (2012) 580-612; (b) M. De Jong, L. Van Ijzendoorn, M. De Voigt, Appl. Phys. Lett. 77 (2000) 2255-2257.